CSIAM Trans. Life Sci.
doi: 10.4208/csiam-ls.SO-2025-0014

Vol. **x**, No. x, pp. 1-34
xx 2025

A Two-Patch Epidemic Model with Prevalence-Dependent Contact Patterns and Migration Rates

Bruno Buonomo* and Emanuela Penitente

Department of Mathematics and Applications, University of Naples Federico II, via Cintia, I-80126 Naples, Italy.

Received 28 May 2025; Accepted 2 August 2025

Dedicated to Prof. Ma Zhien on the occasion of his 90th birthday, with deep gratitude for his thirty-year friendship, his kindness, and the inspiration drawn from his lectures and papers.

Abstract. We consider a two-patch Susceptible-Infected-Recovered epidemic model that incorporates awareness-driven behavioural changes in both contact and mobility patterns. Individuals modify their behaviour in response to a perceived risk of infection, which is modelled through two awareness variables that depend either on the current or past disease prevalence in each patch. We qualitatively analyse the model through stability and bifurcation theory and derive threshold conditions that determine the existence and stability of the biologically relevant equilibria. We find that awareness-induced behavioural changes in contact and mobility can destabilise mixed equilibria – where the disease persists in one patch only – and contribute to the emergence of stable co-endemic states. When awareness depends on past epidemic values, the stability analysis shows that mixed equilibria may lose stability via Hopf bifurcations, depending on the sign of some awareness-related parameters. Finally, the impact of the behaviour-related parameters on the epidemic dynamics is investigated through numerical simulations.

AMS subject classifications: 92D30, 34C60

Key words: Mathematical epidemiology, metapopulation, SIR patch model, nonconstant dispersal, awareness.

1 Introduction

Travels of individuals between different geographical regions play a major role in the dynamics of epidemics [19,35,42]. In a highly interconnected world, human mobility as-

*Corresponding author. *Email addresses:* buonomo@unina.it (B. Buonomo), emanuela.penitente@unina.it (E. Penitente)

sociated with trade, migration, or tourism facilitates the spread of pathogens across heterogeneous environments [56]. Massive and continuous travels between different cities and countries enhanced the spread of the 2003 SARS epidemic [37,46], the 2009 H1N1 influenza pandemic [33,50] and also the global spread of COVID-19 [16,35]. Mathematical modelling, when combined with medical and public health tools, can help to improve the understanding of epidemics in different geographical regions and the development of adequate control strategies [35,42].

Spatial movements of individuals can be modelled in several ways. One approach treats space as a continuous variable, leading to partial differential equation models [1,38,41,44]. In this context, individuals are assumed to move from a given point to their direct neighbourhood. This assumption, suitable for describing phenomena in which the movement of individuals occurs locally and continuously in space, does not fit phenomena involving long-distance movements (e.g. air travel, trade routes, or rapid migrations). Alternatively, modelling space as a discrete variable leads to the so-called metapopulation models, compartmental models in which space is divided into a finite number of patches. A patch can denote a city or a geographic area, and the movements of individuals in space are modelled as dispersal between distinct patches [3,4,38].

Since the 1960s, many researchers have focused on formulating adequate metapopulation models for infectious diseases, and detailed reviews can be found in [3,4,7,37,38] and references therein. In 2003, Wang and Mulone [52] formulated a two-patch susceptible-infected-susceptible (SIS) compartmental model with standard incidence and interpatch movements allowed for both susceptible and infectious individuals. The work addresses the issue of disease persistence, identifying the unity as a sharp threshold of the basic reproduction number that determines whether the disease dies out or persists within the population. Jin and Wang [32], Wang and Zhao [53] considered an n-patch SIS model with susceptible and infectious dispersal, and analysed the effects of migrations on the dynamics of the epidemics. Among the main results, they found that for specific birth functions, population dispersal can lead to the coexistence of multiple endemic equilibria or even multi-stable endemic equilibria if the basic reproduction number is greater than one. In 2010, Yang, Wu, Li and Ma [58] considered a two-patch susceptible-infected-recovered (SIR) model in which the migration of infectious individuals is neglected, as they are considered banned from travelling due to medical screening. Differently to previous works on patch models, the authors focused on the global asymptotic stability of equilibria, rather than on the persistence of the disease. Other contributions on patch models can be found in [5, 6, 8, 31], where compartmental models with more complex structures are formulated.

In recent years, increasing attention has been devoted to developing patch models in which contact or dispersal rates are no longer assumed constant, but are modulated in response to the state of the epidemic. This modelling approach is motivated by the growing influence of social media and digital communication, which can rapidly shape public awareness, risk perception, and individual behaviour. The dissemination of information by public health authorities, together with media-driven awareness campaigns,

can significantly affect both mobility and contact patterns during outbreaks [18, 34, 42]. In light of these considerations, several studies have proposed models in which dispersal or contact rates depend on disease prevalence [36, 47–49, 57].

In 2020, Yang *et al.* [57] studied a two-patch SIS model in which the transmission rates are assumed to be constant, while media coverage negatively affects travel rates of both susceptible and infectious individuals. In 2023, Lu *et al.* [36] considered a two-patch Susceptible-Infected-Recovered-Susceptibles (SIRS) model with both transmission and dispersal rates assumed to be prevalence-dependent. In each patch, the authors considered a transmission rate of the form $\beta_i(I_i) = \beta_i(1+\nu_i I_i), i = 1,2$, where the prevalence-dependent term $\beta_i \nu_i I_i$ expresses a positive feedback caused by an increased risk of infection as the number of infected increases. Moreover, the mobility of susceptible and recovered individuals is modelled as a function of the difference between the relative prevalences in the two patches. In 2024, a couple of two-patch SIR-like models have been studied by Sun *et al.* [48, 49], in which the dispersal of individuals is constant for each compartment and transmission rates are assumed to decrease depending on both present and past values of disease prevalence, to represent the effect of media-driven surveillance on disease transmission and the possibly delayed spread of information. Their results indicate that the model can exhibit Hopf bifurcations when the media-induced disease surveillance is based also on past information.

Most of the aforementioned models account for reductions in contact and travel rates as direct responses to the influence of media. However, awareness is not only due to the amount of information disseminated through the media, but also to how individuals perceive the risk of infection [25]. Therefore, the decision to adopt preventive behaviours is a complex phenomenon that involves several factors, including not only media exposure but also the social, economic and psychological cost of adopting preventive measures [25, 27, 28]. For this reason, the phenomenon studied in this work differs from the ones explored in [36, 47–49, 57], where the direct impact of media coverage on disease transmission is studied.

Motivated by the above discussion, in this work we consider a two-patch epidemic model, based on a previous model by Yang, Wu, Li and Ma [58], and extend it to include the effects of human behavioural changes. More precisely, we assume that the awareness concerning the prevalence of the disease affects the contact patterns within each patch as well as the migration rates between the patches. The awareness about the epidemic status in the i-th patch is quantified by means of an awareness variable $m_i(t), i = 1,2$, that depends on the disease prevalence in patch-i and affects both transmission and travel rates.

We first consider the case in which $m_i(t)$ depends only on the current prevalence in the i-th patch. In other words, we assume that individuals have no memory of past epidemic values and adjust their behaviour solely based on the current state of the outbreak. The resulting model, described by a system of non-linear ordinary differential equations, is qualitatively analysed by using stability and bifurcation theory. We derive conditions for the existence and stability of the biologically relevant steady states, corresponding to scenarios where the disease is either absent in both patches, persists endemically in one

patch only, or is endemic in both. We also examine how behavioural changes affect the stability of the equilibria and impact the overall epidemic size.

Then, we study how memory of past epidemic values affects the formation of awareness. This approach reflects the idea that individuals base their behavioural response not only on the current state of the epidemic, but also on its recent history. As a consequence, we extend the model by assuming that the rate of change of the awareness variable is the balance between two different processes: a production process, represented by a term that depends on disease prevalence in the i-th patch, and a depletion process, reflecting the natural fading of awareness over time due to the limited memory of individuals.

The remainder of this work is structured as follows. In Section 2, we present the mathematical model. Section 3 is dedicated to its qualitative analysis, including the identification of equilibria and the study of their stability properties. In Section 4, we introduce the extended model that incorporates memory effects and investigate the local stability of mixed endemic equilibria, i.e. equilibria where the disease persists in only one of the two patches. Section 5 presents numerical simulations aimed at exploring the impact of the behaviour-related parameters on the epidemic dynamics. Finally, in Section 6, we discuss the main results and give an outlook on possible research perspectives.

2 Model formulation

2.1 State and awareness variables

We consider a spatially structured population divided into two patches, denoted as patch-1 and patch-2. The spread of the epidemic in each patch is described by a classical SIR model, i.e. the population living in each patch is partitioned into three disjoint compartments: susceptible, infected and recovered individuals. The sizes of these compartments at time t, denoted by $S_i(t), I_i(t)$ and $R_i(t), i = 1,2$, are state variables of the model. Their rate of change is ruled by a system of balance equations, mainly based on the above-mentioned paper Yang, Wu, Li and Ma [58].

To model the behavioural changes induced by awareness, we introduce the quantity m_i for $i=1,2$, which represents the level of awareness regarding the disease status in the i-th patch. A similar approach has been previously adopted to model the awareness about respiratory diseases in spatially non-structured populations [34, 43]. The "awareness" variable $m_i(t)$ is assumed to be an increasing function of the prevalence $I_i(t)$ in the i-th patch

$$m_i(t) = g_i\big(I_i(t)\big), \quad i=1,2, \tag{2.1}$$

where $g_i(0)=0, g_i'(I_i)>0$ whenever $I_i>0$. The function g_i quantifies the individuals' risk perception due to the infection in the i-th patch. Examples of suitable functions are a linear function of the disease prevalence, $g_i(I_i) = k_i I_i$, and a Holling II type function $g_i(I_i) = k_i I_i/(1+h_i I_i)$, where $k_i, h_i > 0$. We emphasise that the two functions g_1 and g_2 may have different functional forms, to reflect different perceived risks of contracting the

disease in the two patches. These differences may arise, for example, from variations in variations in disease mortality rates, disparities in healthcare system capacities, or differences in efficiencies in detecting the infected cases.

Remark 2.1. The awareness variable defined in Eq. (2.1) can be interpreted as a particular case of the more general concept of information index, introduced by A. d'Onofrio, P. Manfredi and co-authors in a series of papers starting in 2007 [13, 22, 24]. The information index $M(t)$ is a function that summarises information about the present and past course of the epidemic and captures the population's perception of epidemic risk. It is defined via the following distributed delay equation:

$$M(t)=\int_0^\infty g\big(x_1(t-\tau),x_2(t-\tau),\dots,x_n(t-\tau)\big)\,H(t-\tau)\rho(\tau)d\tau, \tag{2.2}$$

where g is the message function, describing how the population perceives the epidemic risk based on selected model variables. It can depend on some or all the state variables of the model, depending on which quantities are considered as relevant for behavioural changes. The function H is the Heaviside step function, indicating that the perception process starts at the onset of the epidemic (i.e. $t_0=0$), and ρ is a memory kernel, a probability density function weighting the past values of the message function.

By choosing $\rho(\tau)=\delta(\tau)$, where δ is the Dirac delta function, and choosing a prevalence-dependent message function $g_i(t)=g(I_i(t)), i=1,2$, from Eq. (2.2) we can recover the awareness variable $m_i(t), i=1,2$.

2.2 The intra-patch contact rates

Let us denote by β_i and c_i the transmission rate and contact rate in the i-th patch, respectively. Furthermore, denote by π the probability that a contact between a susceptible and an infected individual leads to transmission of the disease.

Individuals in each patch are assumed to voluntarily reduce their interpersonal contacts – through measures such as social distancing, mask-wearing, and so on – depending on their awareness of the epidemic status within their own patch. Therefore, the per capita contact rate c_i in the i-th patch-i depends on the awareness variable m_i. We set

$$c_i(m_i)=\hat{c}_i-c_i^F(m_i), \quad i=1,2, \tag{2.3}$$

where $\hat{c}_i>0$ denotes the per capita contact rate in patch-i in absence of epidemic, which we take as baseline contact rate; and the term $c_i^F(m_i)$ represents the reduction in contact rate induced by the awareness. Note that the superscript F stands for "fear", indicating the behavioural response driven by risk perception. We require that the function c_i^F satisfies the following properties: (i) it is an increasing function of m_i, (ii) $c_i^F(0)=0$, (iii) $\max\big(c_i^F(m_i)\big)<\hat{c}_i$.

Since the transmission rate β_i is the product of the contact rate c_i times the probability π of getting infected after contact with an infectious individual, the awareness-dependent transmission rate is

$$\beta_i(m_i) = \hat{\beta}_i - \beta_i^F(m_i), \tag{2.4}$$

where $\hat{\beta}_i$ denotes the "baseline" transmission rate in the i-th patch, and $\beta_i^F(m_i)$ is the awareness-dependent part of the transmission rate.

2.3 The inter-patch travel rates

We assume that individuals from patch-i travel to patch-j, with $i,j=1,2$ and $i \neq j$, at rates that depend on their disease status, which remains unchanged during travels. The parameter a_i denotes the rate at which susceptible individuals from patch-i move to patch-j, whereas b_i represents the analogous travel rate for recovered individuals. We also assume that infected individuals do not migrate between the two patches, that is, the migration rates of infected individuals are considered negligible. This modelling choice makes the analysis more manageable, while still providing meaningful insights into the system's dynamics. A possible interpretation is related to diseases causing severe symptoms (such as measles, SARS-CoV-1, etc.) where infected individuals are physically unable to travel or they have very limited travel patterns [45, 55]. Additionally, this assumption implicitly accounts for containment strategies, such as isolation or quarantine, which primarily involve the mobility of infected individuals.

The rate a_i is assumed to depend on awareness, reflecting behavioural changes driven by the perceived risk of infection. In contrast, the rate b_i is assumed to be constant, as recovered individuals are immune and no longer influenced by the fear of becoming infected. To model the awareness-dependent travel rate a_i, we assume that it depends on both the awareness variables, reflecting that individuals can adjust their mobility behaviour not only depending on the perceived risk of infection in the destination patch, but rather by comparing the levels of awareness between the two patches. This behavioural mechanism has been recently adopted to model the prevalence-based mobility in epidemic patch models [36]. We set the awareness-dependent travel rate as

$$a_i(m_1,m_2) = a_i(z_i), \quad z_i(m_1,m_2) = \theta_i(m_i - m_j), \quad i,j=1,2, \quad i \neq j. \tag{2.5}$$

The parameter $\theta_i \in [0,1]$, referred to as the mobility responsiveness parameter, quantifies the degree to which the epidemic awareness influences the mobility of susceptibles living in the i-th patch. We require that the function $a_i(z_i)$ satisfies the following assumptions:

(i) $a_i(0) = \hat{a}_i$, where $\hat{a}_i > 0$ represents the travel rate from the i-th patch in absence of epidemic, that we take as baseline travel rate;

(ii) a_i is an increasing function of z_i;

(iii) $a_i(z_i)$ is nonnegative in its domain.

Condition (i) ensures that, when the awareness levels m_1 and m_2 are equal, individuals maintain their usual travel patterns, as if no epidemic were present. Condition (ii) implies that the travel rate a_i increases with the awareness m_i in the origin patch and decreases with the awareness m_j in the destination patch, reflecting the propensity of people to move out from high-risk areas and to avoid entering them.

The specific functional forms of the transmission rates β_1 and β_2, as well as those of the travel rates a_1 and a_2, will be specified in Section 5.1. The dynamics of the two-patch subsystem are illustrated in the flowchart in Figure 1.

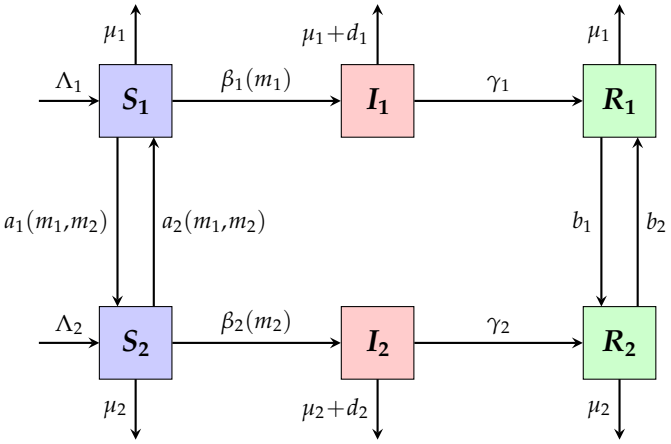

Figure 1: Flowchart of the model (2.6).

2.4 The balance equations

The awareness-based metapopulation model, inspired by the one introduced by Yang, Wu, Li, and Ma [58], is governed by the following system of ordinary differential equations:

$$
\begin{aligned}
\dot{S}_1(t) &= \Lambda_1 - \mu_1 S_1 - \beta_1(m_1) S_1 I_1 - a_1(m_1,m_2) S_1 + a_2(m_1,m_2) S_2,\\
\dot{I}_1(t) &= \beta_1(m_1) S_1 I_1 - (\mu_1+\gamma_1+d_1) I_1,\\
\dot{R}_1(t) &= \gamma_1 I_1 - \mu_1 R_1 - b_1 R_1 + b_2 R_2,\\
\dot{S}_2(t) &= \Lambda_2 - \mu_2 S_2 - \beta_2(m_2) S_2 I_2 + a_1(m_1,m_2) S_1 - a_2(m_1,m_2) S_2,\\
\dot{I}_2(t) &= \beta_2(m_2) S_2 I_2 - (\mu_2+\gamma_2+d_2) I_2,\\
\dot{R}_2(t) &= \gamma_2 I_2 - \mu_2 R_2 + b_1 R_1 - b_2 R_2,
\end{aligned}
$$

where the upper dots denote the time derivatives and the rates $\beta_i(m_i), a_i(m_1,m_2)$ are given by Eqs. (2.1), (2.3) and (2.5). The parameters Λ_i, μ_i, d_i and γ_i are assumed to be positive constants with the following interpretations: they are the rates of recruitment, natural death, disease–induced death and recovery in the i-th patch, respectively. Since

the balance equations for R_1 and R_2 are uncoupled from the remaining ones, we consider the following subsystem:

$$\dot{S}_1(t) = \Lambda_1 - \mu_1 S_1 - \beta_1(m_1) S_1 I_1 - a_1(m_1,m_2) S_1 + a_2(m_1,m_2) S_2, \tag{2.6a}$$
$$\dot{I}_1(t) = \beta_1(m_1) S_1 I_1 - \varepsilon_1 I_1, \tag{2.6b}$$
$$\dot{S}_2(t) = \Lambda_2 - \mu_2 S_2 - \beta_2(m_2) S_2 I_2 + a_1(m_1,m_2) S_1 - a_2(m_1,m_2) S_2, \tag{2.6c}$$
$$\dot{I}_2(t) = \beta_2(m_2) S_2 I_2 - \varepsilon_2 I_2, \tag{2.6d}$$

where $\varepsilon_i = \mu_i + \gamma_i + d_i, i = 1,2$. The system is equipped with the following initial conditions:

$$S_i(0) > 0, \quad I_i(0) \geq 0, \quad i = 1,2. \tag{2.7}$$

The total population $N(t)$ living in both patches is given by $N(t) = N_1(t) + N_2(t)$, where $N_i(t) = S_i(t) + I_i(t), i = 1,2$, denotes the total population living in patch-i at time t.

Finally, note that system (2.6)-(2.7) can be rewritten in the vectorial form

$$\dot{\mathbf{x}}(t) = \mathbf{F}\big(\mathbf{x}(t)\big), \quad \mathbf{x}(0) = \mathbf{x}_0,$$
$$\mathbf{x}(t) = (x_i(t))_{i=1,\dots,4} = \big(S_1(t), I_1(t), S_2(t), I_2(t)\big),$$

and $\mathbf{F}(\mathbf{x}) = (f_1(\mathbf{x}), f_2(\mathbf{x}), f_3(\mathbf{x}), f_4(\mathbf{x}))$ is the autonomous vector field.

3 Mathematical analysis

3.1 Biologically feasible region

Lemma 3.1. *Assume that the initial condition $\mathbf{x}_0$ of model (2.6) has all strictly positive components. Then, the solution $\mathbf{x}(t)$ has all strictly positive components for any $t > 0$.*

Proof. See Appendix A. □

Proposition 3.1. *The solution of the Cauchy problem (2.6)-(2.7) exists, is unique in the interval $[0,\infty)$ and is contained in the positively invariant and attractive set Ω defined by*

$$\Omega = \left\{ \mathbf{x} \in \mathbb{R}^4_+ : \sum_{i=1}^{4} x_i \leq \frac{\Lambda_1 + \Lambda_2}{\min\{\mu_1, \mu_2\}} \right\},$$

where $\mathbb{R}^4_+$ is the non-negative orthant of $\mathbb{R}^4$.

Proof. See Appendix A. □

3.2 Reproduction numbers and disease extinction

Model (2.6) admits a unique disease-free equilibrium

$$E_0 = \left(S_1^{(0)},0,0,S_2^{(0)},0,0\right),$$

where

$$S_1^{(0)} = \frac{\Lambda_1(\mu_2+\hat{a}_2)+\Lambda_2\hat{a}_2}{\mu_1\mu_2+\mu_1\hat{a}_2+\mu_2\hat{a}_1}, \qquad S_2^{(0)} = \frac{\Lambda_2(\mu_1+\hat{a}_1)+\Lambda_1\hat{a}_1}{\mu_1\mu_2+\mu_1\hat{a}_2+\mu_2\hat{a}_1}.$$

We analyse the stability of the disease-free equilibrium in terms of the basic reproduction number $\mathcal{R}_0$, defined as the average number of secondary cases produced by an infected individual in a fully susceptible population over the full course of the infectious period [20]. An explicit expression for $\mathcal{R}_0$ is derived using the method of next-generation matrix (NGM), introduced by Diekmann *et al.* [20] and van den Driessche and Watmough [51].

We denote by $\mathcal{F}$ the vector of new infection rates into the infected compartments

$$\mathcal{F}(\mathbf{x}) = \begin{bmatrix}\beta_1(m_1)S_1I_1\\ \beta_2(m_2)S_2I_2,\end{bmatrix},$$

and denote by $\mathcal{V}$ the vector of the outflows from the infected compartments due to all other processes (recovery, death or travel)

$$\mathcal{V}(\mathbf{x}) = \begin{bmatrix}\varepsilon_1 I_1\\ \varepsilon_2 I_2\end{bmatrix}.$$

The Jacobian of $\mathcal{F}$ and $\mathcal{V}$, evaluated at E_0, are the so-called transmission matrix F and the transition matrix V [21]

$$F = \begin{bmatrix}\beta_1(0)S_1^{(0)} & 0\\ 0 & \beta_2(0)S_2^{(0)}\end{bmatrix}, \quad V = \begin{bmatrix}\varepsilon_1 & 0\\ 0 & \varepsilon_2\end{bmatrix}. \tag{3.1}$$

The basic reproduction number $\mathcal{R}_0$ is the spectral radius of the NGM, given by

$$\text{NGM} = FV^{-1} = \begin{bmatrix}\dfrac{\beta_1(0)S_1^{(0)}}{\varepsilon_1} & 0\\ 0 & \dfrac{\beta_2(0)S_2^{(0)}}{\varepsilon_2}\end{bmatrix}.$$

Denoting by

$$\mathcal{R}_{01} = \frac{\beta_1(0)S_1^{(0)}}{\varepsilon_1} = \frac{\hat{\beta}_1[\Lambda_1(\mu_2+\hat{a}_2)+\Lambda_2\hat{a}_2]}{\varepsilon_1(\mu_1\mu_2+\mu_1\hat{a}_2+\mu_2\hat{a}_1)}, \tag{3.2}$$

$$\mathcal{R}_{02} = \frac{\beta_2(0)S_2^{(0)}}{\varepsilon_2} = \frac{\hat{\beta}_2[\Lambda_2(\mu_1+\hat{a}_1)+\Lambda_1\hat{a}_1]}{\varepsilon_2(\mu_1\mu_2+\mu_1\hat{a}_2+\mu_2\hat{a}_1)}, \tag{3.3}$$

we get that $\mathcal{R}_0 = \max\{\mathcal{R}_{01},\mathcal{R}_{02}\}$.

The parameter $\mathcal{R}_{0i}$ for $i=1,2$, is the basic reproduction number of the disease in the i-th patch, $i=1,2$, when dispersal occurs between the patches and the other patch is at the disease-free steady state. The expression of $\mathcal{R}_{0i}$ is consistent with the classical epidemiological interpretation of the basic reproduction number, as it is given by the product of the transmission rate in the i-th patch, the average duration of the infectious period, and the number of susceptible individuals in the i-th patch at the disease-free equilibrium.

It is worth to note that in models incorporating awareness-driven behavioural changes, the basic reproduction number $\mathcal{R}_0$ may have limited epidemiological significance. Behavioural responses can dynamically alter contact patterns and transmission rates, causing the trajectory of the system to diverge from the assumptions underlying a fixed $\mathcal{R}_0$. In such contexts, the effective reproduction number $\mathcal{R}(t)$, which evolves with time and behaviour, may offer a more accurate picture of transmission potential.

However, estimating $\mathcal{R}(t)$ can be particularly difficult in practice, as it requires high-quality incidence data, accurate knowledge of the generation interval, and careful adjustment for reporting delays and under-detection [17,26,29]. These challenges are especially pronounced in models with feedback between behaviour and transmission. Therefore, while $\mathcal{R}(t)$ offers more realism in principle, $\mathcal{R}_0$ remains a valuable theoretical tool, and we use it for comparison between scenarios and threshold analysis.

Proposition 3.2. *If $\mathcal{R}_0<1$, the disease-free equilibrium E_0 of model* (2.6) *is locally asymptotically stable. If $\mathcal{R}_0>1$, then E_0 is unstable.*

Proof. The well-known NGM method described in [51, Theorem 2], is based on five conditions that are trivially satisfied in our case, except for the condition denoted as (A5) in [51], which requires that if $\mathcal{F}$ is set to zero, then all the eigenvalues of the Jacobian matrix $J(E_0)$ must have negative real parts. However, it is easy to check that the first two eigenvalues of $J(E_0)$ are $\lambda_1=-\varepsilon_1$ and $\lambda_2=-\varepsilon_2$. The remaining eigenvalues correspond to those of the submatrix

$$J_0=\begin{bmatrix}-\mu_1-\hat{a}_1 & \hat{a}_2\\ \hat{a}_1 & -\mu_2-\hat{a}_2\end{bmatrix}.$$

Since $\mathrm{tr}(J_0)<0$ and $\det(J_0)>0$, the eigenvalues of J_0 have negative real parts, implying that E_0 is locally asymptotically stable when $\mathcal{R}_0<1$. □

When the patches are disconnected, the corresponding basic reproduction number in each patch reduces to $\mathcal{B}_{0i}=(\hat{\beta}_i\Lambda_i)/(\varepsilon_i\mu_i)$. We can easily derive the following relationships between R_{0i} and B_{0i}:

- If $\Lambda_1\hat{a}_1\mu_2<\Lambda_2\hat{a}_2\mu_1$, then $\mathcal{R}_{01}>\mathcal{B}_{01}$ and $\mathcal{R}_{02}<\mathcal{B}_{02}$.
- If $\Lambda_1\hat{a}_1\mu_2>\Lambda_2\hat{a}_2\mu_1$, then $\mathcal{R}_{01}<\mathcal{B}_{01}$ and $\mathcal{R}_{02}>\mathcal{B}_{02}$.

Since one of the two inequalities must necessarily hold, the mobility promotes disease transmission in one of the two patches while mitigating it in the other. In addition, even if

$\max\{\mathcal{B}_{01},\mathcal{B}_{02}\}<1$ (i.e. the disease dies out in each patch when disconnected), for suitable travel rates we may have either $\mathcal{R}_{01}>1$ or $\mathcal{R}_{02}>1$, implying that $\mathcal{R}_0>1$ and the epidemic takes place in the connected environment.

Assume now that the travel rates do not depend on awareness. We derive the global asymptotic stability of E_0 when $\mathcal{R}_0<1$.

Proposition 3.3. *Assume that $a_i(m_1,m_2)=\hat{a}_i$, $i=1,2$. If $\mathcal{R}_0<1$, then the disease-free equilibrium E_0 is globally asymptotically stable in Ω.*

Proof. The local stability of E_0 for $\mathcal{R}_0<1$ follows from Proposition 3.2. We claim that if $\mathcal{R}_0<1$, the equilibrium E_0 is globally attractive. By the positive invariance of $\mathbb{R}^4_+$ and from (2.6a) and (2.6c), we derive

$$\begin{aligned}\dot{S}_1(t)&\leq\Lambda_1-\mu_1S_1-\hat{a}_1S_1+\hat{a}_2S_2,\\ \dot{S}_2(t)&\leq\Lambda_2-\mu_2S_2+\hat{a}_1S_1-\hat{a}_2S_2.\end{aligned}$$

Defining the auxiliary linear system

$$\begin{aligned}s_1'(t)&=\Lambda_1-\mu_1s_1-\hat{a}_1s_1+\hat{a}_2s_2,\\ s_2'(t)&=\Lambda_2-\mu_2s_2+\hat{a}_1s_1-\hat{a}_2s_2\end{aligned}\tag{3.4}$$

with initial conditions $(s_1(0),s_2(0))=(S_1(0),S_2(0))$, the comparison principle yields $S_i(t)\leq s_i(t)$ for $t\geq 0, i=1,2$. System (3.4) admits $(S_1^{(0)},S_2^{(0)})$ as globally asymptotically stable equilibrium, i.e.

$$\lim_{t\to\infty}\big(s_1(t),s_2(t)\big)=\big(S_1^{(0)},S_2^{(0)}\big)$$

for any initial data $(S_1(0),S_2(0))\in\Omega$. It follows that for any given $\delta>0$, there exists a $T>0$ such that

$$\begin{aligned}S_1(t)\leq s_1(t)\leq S_1^{(0)}+\delta,\\ S_2(t)\leq s_2(t)\leq S_2^{(0)}+\delta,\end{aligned}\quad t>T.\tag{3.5}$$

By applying the inequalities in (3.5) to Eqs. (2.6b) and (2.6d) and noting that $\beta_i(m_i)\leq\hat{\beta}_i$, we obtain

$$\begin{aligned}\dot{I}_1(t)&\leq I_1\big[\hat{\beta}_1\big(S_1^{(0)}+\delta\big)-\varepsilon_1\big],\\ \dot{I}_2(t)&\leq I_2\big[\hat{\beta}_2\big(S_2^{(0)}+\delta\big)-\varepsilon_2\big],\end{aligned}\quad t>T.$$

We define the following auxiliary system:

$$\begin{aligned}i_1'(t)&\leq i_1\big[\hat{\beta}_1\big(S_1^{(0)}+\delta\big)-\varepsilon_1\big],\\ i_2'(t)&\leq i_2\big[\hat{\beta}_2\big(S_2^{(0)}+\delta\big)-\varepsilon_2\big],\end{aligned}\tag{3.6}$$

that in vectorial form is $(d/dt)(i_1,i_2)=(F-V+\delta D)(i_1,i_2)$ with $D=\mathrm{diag}(\hat{\beta}_1,\hat{\beta}_2)$.

From [51], the condition $\mathcal{R}_0<1$ holds if and only if the eigenvalues of $F-V$ have negative real parts, where the matrices F and V are given by Eq. (3.1). Since the spectrum of a matrix depends continuously on its entries, all the eigenvalues of $F-V+\delta D$ have negative real parts for δ sufficiently small. This shows that the equilibrium $(0,0)$ is globally asymptotically stable for the linear system (3.6). Thus, by the comparison principle,

$$\lim_{t\to\infty} I_i(t)=0, \quad i=1,2.$$

This shows that system (3.4) is a limiting system for model (2.6). By the theory of asymptotically autonomous systems [15], the disease-free equilibrium E_0 of model (2.6) is globally asymptotically stable for $\mathcal{R}_0<1$. □

If the travel rate $a_i, i=1,2$, depends on the awareness variables m_1 and m_2, a stronger condition is required to ensure the global stability of E_0. Preliminarily, we introduce the following parameter:

$$\mathcal{R}_0^{\text{gas}} := \frac{\max\{\hat{\beta}_1,\hat{\beta}_2\}}{\min\{\varepsilon_1,\varepsilon_2\}}\frac{\Lambda_1+\Lambda_2}{\min\{\mu_1,\mu_2\}}. \tag{3.7}$$

Theorem 3.1. *If $\mathcal{R}_0^{\text{gas}}<1$, then the disease-free equilibrium E_0 of model* (2.6) *is globally asymptotically stable in Ω.*

Proof. Adding Eqs. (2.6b) and (2.6d) yields

$$\begin{aligned}\dot{I}_1(t)+\dot{I}_2(t) &= \beta_1(m_1)S_1I_1+\beta_2(m_2)S_2I_2-\varepsilon_1I_1-\varepsilon_2I_2\\ &\le \beta_1(m_1)S_1(I_1+I_2)+\beta_2(m_2)S_2(I_1+I_2)-\min\{\varepsilon_1,\varepsilon_2\}(I_1+I_2)\\ &\le (I_1+I_2)[\hat{\beta}_1S_1+\hat{\beta}_2S_2-\min\{\varepsilon_1,\varepsilon_2\}]\\ &\le (I_1+I_2)[\max\{\hat{\beta}_1,\hat{\beta}_2\}(S_1+S_2)-\min\{\varepsilon_1,\varepsilon_2\}].\end{aligned}$$

Using that

$$S_1+S_2\le\frac{\Lambda_1+\Lambda_2}{\min\{\mu_1,\mu_2\}}-(I_1+I_2),$$

leads to following inequality:

$$\begin{aligned}\frac{d}{dt}\big(I_1(t)+I_2(t)\big)\le&\left[\max\{\hat{\beta}_1,\hat{\beta}_2\}\frac{\Lambda_1+\Lambda_2}{\min\{\mu_1,\mu_2\}}-\min\{\varepsilon_1,\varepsilon_2\}\right](I_1+I_2)\\ &-\max\{\hat{\beta}_1,\hat{\beta}_2\}(I_1+I_2)^2.\end{aligned}$$

If $\mathcal{R}_0^{\text{gas}}<1$, the function $I_1(t)+I_2(t)$ is nonnegative and monotonically decreasing for $t>0$. Thus,

$$\lim_{t\to\infty} I_i(t)=0, \quad i=1,2.$$

This shows that the system

$$\dot{s}_1(t) = \Lambda_1 - \mu_1 s_1 - \hat{a}_1 s_1 + \hat{a}_2 s_2,$$
$$\dot{s}_2(t) = \Lambda_2 - \mu_2 s_2 + \hat{a}_1 s_1 - \hat{a}_2 s_2$$

is a limiting system for model (2.6). Therefore, by the theory of asymptotically autonomous systems, the equilibrium E_0 is globally asymptotically stable if $\mathcal{R}_0^{\text{gas}} < 1$. □

The condition $\mathcal{R}_0^{\text{gas}} < 1$ in the statement of Theorem 3.1 is stronger than $\mathcal{R}_0 < 1$ since, from $S_1^{(0)} + S_2^{(0)} < (\Lambda_1 + \Lambda_2)/\min\{\mu_1, \mu_2\}$, we get

$$\begin{aligned}\mathcal{R}_0 :&= \max\left\{\frac{\hat{\beta}_1}{\varepsilon_1} S_1^{(0)}, \frac{\hat{\beta}_2}{\varepsilon_2} S_2^{(0)}\right\} \leq \max\left\{\frac{\hat{\beta}_1}{\varepsilon_1}, \frac{\hat{\beta}_2}{\varepsilon_2}\right\} \max\left\{S_1^{(0)}, S_2^{(0)}\right\} \\ &\leq \frac{\max\{\hat{\beta}_1, \hat{\beta}_2\}}{\min\{\varepsilon_1, \varepsilon_2\}} \left(S_1^{(0)} + S_2^{(0)}\right) \\ &\leq \frac{\max\{\hat{\beta}_1, \hat{\beta}_2\}}{\min\{\varepsilon_1, \varepsilon_2\}} \frac{\Lambda_1 + \Lambda_2}{\min\{\mu_1, \mu_2\}} = \mathcal{R}_0^{\text{gas}}.\end{aligned}$$

Remark 3.1. It is also important to note that both the coordinates of the disease-free equilibrium E_0 and its local stability are not affected by the awareness variables $m_i, i = 1,2$. Moreover, although a stronger condition is required to ensure the global stability of E_0 when travel rates depend on awareness (Theorem 3.1), the stability threshold is independent of the specific functional form of the functions $m_i(t)$. In Section 4, we will consider a model where $m_i(t)$ depends on the past values of epidemics. Of course, the stability analysis of E_0 carried out in this section will also hold for that model.

3.3 Endemic equilibria and local stability

Model (2.6) admits two mixed equilibria, E_1 and E_2, representing steady states in which the disease is endemic in one patch only, while the other is disease-free. The equilibrium $E_1 = (S_1^*, I_1^*, S_2^*, 0)$ have coordinates

$$S_1^* = \frac{\varepsilon_1}{\beta_1(m_1^*)}, \quad S_2^* = \frac{1}{\mu_2 + a_2(m_1^*, 0)} \left(\Lambda_2 + \frac{a_1(m_1^*, 0)\varepsilon_1}{\beta_1(m_1^*)}\right), \quad m_1^* = g_1(I_1^*), \tag{3.8}$$

where I_1^* is the unique positive root of the function

$$\xi_1(x) = \frac{\Lambda_1}{\varepsilon_1} - \frac{\mu_1 + a_1(g_1(x), 0)}{\beta_1(g_1(x))} + \frac{a_2(g_1(x), 0)}{\mu_2 + a_2(g_1(x), 0)} \left[\frac{\Lambda_2}{\varepsilon_1} + \frac{a_1(g_1(x), 0)}{\beta_1(g_1(x))}\right] - x.$$

Since ξ_1 is monotonically decreasing in x and $f_1(0) > 0$ if and only if $\mathcal{R}_{01} > 1$, the equilibrium E_1 exists if and only if $\mathcal{R}_{01} > 1$.

Analogously, the coordinates of $E_2=(S_1^{**},0,S_2^{**},I_2^{**})$ are positive if and only if $\mathcal{R}_{02}>1$ and are given by

$$S_1^{**}=\frac{1}{\mu_1+a_1(0,m_2^{**})}\left(\Lambda_1+\frac{a_2(0,m_2^{**})\varepsilon_2}{\beta_2(m_2^{**})}\right),\quad S_2^{**}=\frac{\varepsilon_2}{\beta_2(m_2^{**})},\quad m_2^{**}=g_2(I_2^{**}),$$

where I_2^{**} is the unique positive root of

$$\xi_2(y)=\frac{\Lambda_2}{\varepsilon_2}-\frac{\mu_2+a_2\big(0,g_2(y)\big)}{\beta_2\big(g_2(y)\big)}+\frac{a_2\big(0,g_2(y)\big)}{\mu_1+a_1\big(0,g_2(y)\big)}\left[\frac{\Lambda_1}{\varepsilon_2}+\frac{a_2\big(0,g_2(y)\big)}{\beta_2\big(g_2(y)\big)}\right]-y.$$

In the unresponsive scenario, where individuals do not adapt their behaviour in response to the epidemic (i.e. the functions $c_i^F(m_i)$ and $z(m_1,m_2)$, defined in Eqs. (2.3) and (2.5), are identically zero), both transmission and travel rates remain constant. Under these conditions, the dynamics reduce to those analysed in Yang, Wu, Li and Ma [58]. The endemic equilibrium in which the disease persists only in the first patch, denoted by $E_1=(S_1^*,I_1^*,S_2^*,0)$, admits the following expression:

$$S_1^*=\frac{\varepsilon_1}{\hat\beta_1},\quad I_1^*=\frac{\Lambda_1(\mu_2+\hat a_2)+\hat a_2\Lambda_2}{\varepsilon_1(\mu_2+\hat a_2)}\left(1-\frac{1}{\mathcal{R}_{01}}\right),\quad S_2^*=\frac{1}{\mu_2+\hat a_2}\left(\Lambda_2+\hat a_1\frac{\varepsilon_1}{\hat\beta_1}\right).$$

Compared to the unresponsive scenario, in the responsive scenario, where awareness modulates transmission and mobility, the behavioural changes lead to a lower transmission rate and reduced travel towards the infected patch, while increasing travel in the opposite direction. In other words, since $\beta_1(m_1)$ and $a_2(m_1,m_2)$ decrease with m_1 and $a_1(m_1,m_2)$ increases with m_1, it follows that

$$\hat\beta_1>\beta_1(m_1^*),\quad a_1(m_1^*,0)>\hat a_1,\quad a_2(m_1^*,0)<\hat a_2.$$

As a result, the equilibrium E_1 under behavioural response is characterised by a higher number of susceptible individuals in both patches and a lower number of infected individuals. This highlights the mitigating role of awareness-driven behaviour in reducing disease prevalence and limiting epidemic spread.

We study the local stability of the equilibrium E_1 by introducing the following parameter:

$$\mathcal{P}_2=\frac{\hat\beta_2 S_2^*}{\varepsilon_2}=\frac{\hat\beta_2}{(\mu_2+a_2^*)\varepsilon_2}\left(\Lambda_2+a_1^*\frac{\varepsilon_1}{\beta_1^*}\right),\tag{3.9}$$

where $\beta_1^*:=\beta_1(m_1^*)$ and $a_i^*:=a_i(m_1^*,0)$, for $i=1,2$, are shortened notations for the transmission and travel rates evaluated at equilibrium E_1. The parameter $\mathcal{P}_2$ is the basic reproduction number in patch-2 when patch-1 is at the endemic steady state [58], and it can be interpreted as the average number of secondary infections produced by one infectious individual living in patch-2 during its lifetime as infectious, given that the disease is endemic in patch-1. In the following proposition, we show that the reproduction number $\mathcal{P}_2$ determines whether the disease will spread or die out in patch-2, given that it is already endemic in patch-1.

Theorem 3.2. *Let $\mathcal{R}_{01}>1$. If $\mathcal{P}_2<1$, then the equilibrium E_1 is locally asymptotically stable. If $\mathcal{P}_2>1$, then the equilibrium E_1 is unstable.*

Proof. By linearising system (2.6) at the equilibrium E_1, we get the characteristic equation $\det(\lambda \mathrm{I}-J(E_1))=0$, i.e.

$$\begin{vmatrix} \lambda+\mu_1+a_1^*+d_3 & \varepsilon_1+d_1-d_4 & -a_2^* & -d_2 \\ -d_3 & \lambda+d_4 & 0 & 0 \\ -a_1^* & -d_1 & \lambda+\mu_2+a_2^* & \hat{\beta}_2 S_2^*+d_2 \\ 0 & 0 & 0 & \lambda+\varepsilon_2-\hat{\beta}_2 S_2^* \end{vmatrix}=0,$$

where

$$\begin{aligned} &d_1=g_1'(I_1^*)\left[\frac{\partial a_1(m_1^*,0)}{\partial m_1}S_1^*-\frac{\partial a_2(m_1^*,0)}{\partial m_1}S_2^*\right]>0, \quad d_3=\beta_1^* I_1^*>0, \\ &d_2=g_2'(0)\left[\frac{\partial a_2(m_1^*,0)}{\partial m_2}S_2^*-\frac{\partial a_1(m_1^*,0)}{\partial m_2}S_1^*\right]>0, \quad d_4=-g_1'(I_1^*)\beta_1'(m_1^*)S_1^* I_1^*>0. \end{aligned} \tag{3.10}$$

Note that (i) $d_i>0, i=1,2$, since the travel rate $a_i(m_i,m_j)$ monotonically increases in m_i and decreases in m_j; (ii) $d_4>0$, since $\beta_1(m_1)$ is monotonically decreasing in m_1.

Obviously, one root of the characteristic equation is $\lambda_4=\mathcal{P}_2-1$. Adding the second and third rows to the first, we obtain

$$\begin{vmatrix} \lambda+\mu_1 & \varepsilon_1+\lambda & \lambda+\mu_2 \\ -\beta_1^* I_1^* & \lambda+d_4 & 0 \\ -a_1^* & -d_1 & \lambda+\mu_2+a_2^* \end{vmatrix}=0,$$

that is,

$$\lambda^3+\mathcal{A}_1\lambda^2+\mathcal{A}_2\lambda+\mathcal{A}_3=0,$$

where

$$\begin{aligned} &\mathcal{A}_1=\mu_1+\mu_2+a_1^*+a_2^*+d_3+d_4, \\ &\mathcal{A}_2=d_3(d_1+\varepsilon_1+a_2^*+\mu_2)+d_4(a_1^*+a_2^*+\mu_1+\mu_2)+\mu_1 a_2^*+\mu_2 a_1^*+\mu_1\mu_2, \\ &\mathcal{A}_3=d_3(\mu_2 d_1+a_2^*\varepsilon_1+\mu_2\varepsilon_1)+d_4(\mu_1 a_2^*+\mu_2 a_1^*+\mu_1\mu_2). \end{aligned}$$

From the Routh-Hurwitz criterion [41, 44], the roots of the characteristic equation have negative real parts if and only if the following conditions hold: (i) $\mathcal{A}_1>0$, (ii) $\mathcal{A}_3>0$ and (iii) $\mathcal{A}_1\mathcal{A}_2>\mathcal{A}_3$. Conditions (i)-(ii) are trivially satisfied. As for condition (iii), we observe that

$$\begin{aligned} \mathcal{A}_1\mathcal{A}_2 &> (\mu_2+a_2^*+d_4)[d_3(d_1+\varepsilon_1)+(\mu_1 a_2^*+\mu_2 a_1^*+\mu_1\mu_2)] \\ &> d_3(\mu_2+a_2^*)(d_1+\varepsilon_1)+d_4(\mu_1 a_2^*+\mu_2 a_1^*+\mu_1\mu_2)>\mathcal{A}_3. \end{aligned}$$

This proves that the equilibrium E_1 is locally asymptotically stable when $\mathcal{P}_2<1$. □

Remark 3.2. In the unresponsive scenario, the reproduction number in patch-2 when patch-1 is at the endemic steady state reduces to

$$\hat{\mathcal{P}}_2 := \frac{\hat{\beta}_2}{(\mu_2+\hat{a}_2)\varepsilon_2}\left(\Lambda_2+\hat{a}_1\frac{\varepsilon_1}{\hat{\beta}_1}\right),$$

where the hat indicates that the quantity refers to the unresponsive scenario. Since $\beta_1(m_1)$ and $a_2(m_1,m_2)$ are decreasing functions of m_1, while $a_1(m_1,m_2)$ increases with m_1, it follows that

$$\mathcal{P}_2 > \hat{\mathcal{P}}_2. \tag{3.11}$$

Then, the behavioural changes induced by awareness of the epidemic in patch-1 lead to an increase in the reproduction number $\mathcal{P}_2$ in patch-2. This can be explained as follows: If individuals react to the awareness of the epidemic, the transmission rate β_1^* in patch-1 decreases. This leads to fewer infections in patch-1 and to a higher number S_1^* of susceptible individuals at the endemic steady state. At the same time, awareness modifies mobility patterns: The travel rate a_1^* from patch-1 increases, while the travel rate a_2^*. As a result, more susceptibles accumulate in patch-2, increasing the average number of new infections produced by a single infectious individual. This results in a higher reproduction number $\mathcal{P}_2$ compared to the unresponsive scenario.

The inequality (3.2) implies that, for suitable parameter values, we may have $\hat{\mathcal{P}}_2 < 1 < \mathcal{P}_2$. In other words, the equilibrium E_1 may be stable in the unresponsive scenario and lose stability in the responsive scenario, where individuals adjust their contact and mobility behaviour in response to awareness. A numerical example illustrating this phenomenon will be provided in Section 5.3.

The stability of the mixed equilibrium E_2 can be obtained by using the same arguments adopted to prove the stability result of E_1. Therefore, we introduce the basic reproduction number in patch-1 when patch-2 is at the endemic steady state

$$\mathcal{P}_1 = \frac{\hat{\beta}_1 S_1^{**}}{\varepsilon_1} = \frac{\hat{\beta}_1}{(\mu_1+a_1^{**})\varepsilon_1}\left(\Lambda_1+a_2^{**}\frac{\varepsilon_2}{\beta_2^{**}}\right),$$

where $\beta_2^{**} := \beta_2(m_2^{**})$ and $a_i^{**} := a_i(0,m_2^{**})$, for $i = 1,2$, are shortened notations for the transmission and travel rates evaluated at equilibrium E_2. The following stability result holds.

Proposition 3.4. *Let $\mathcal{R}_{02} > 1$. If $\mathcal{P}_1 < 1$, then the equilibrium E_2 is locally asymptotically stable. If $\mathcal{P}_1 > 1$, then the equilibrium E_2 is unstable.*

Obviously, the argument of Remark 3.2 also applies to the equilibrium E_2, leading to the following relationship:

$$\mathcal{P}_1 > \hat{\mathcal{P}}_1. \tag{3.12}$$

Proposition 3.5. *Let $\mathcal{R}_{01}, \mathcal{R}_{02} > 1$. The equilibria E_1 and E_2 cannot be both stable for the same parameter values.*

Proof. Assume that E_1 is locally stable, that is, $\mathcal{P}_2<1$. Then, from Eq. (3.11), it follows that $\hat{\mathcal{P}}_2<1$. We now show that $\hat{\mathcal{P}}_1>1$. As a consequence, Eq. (3.12) implies $\mathcal{P}_1>1$, and hence, by Proposition 3.4, the equilibrium E_2 is unstable.

Assume, by contradiction, that both $\hat{\mathcal{P}}_1<1$ and $\hat{\mathcal{P}}_2<1$. By definition, it follows that

$$\begin{cases} \Lambda_2\hat{\beta}_1\hat{\beta}_2+\varepsilon_1\hat{a}_1\hat{\beta}_2<\varepsilon_2(\mu_2+\hat{a}_2)\hat{\beta}_1, & \text{(3.13a)}\\ \Lambda_1\hat{\beta}_1\hat{\beta}_2+\varepsilon_2\hat{a}_2\hat{\beta}_1<\varepsilon_1(\mu_1+\hat{a}_1)\hat{\beta}_2. & \text{(3.13b)}\end{cases}$$

Adding inequalities (3.13a) and (3.13b) leads to

$$\hat{\beta}_1(\Lambda_1\hat{\beta}_2-\mu_2\varepsilon_2)+\hat{\beta}_2(\Lambda_2\hat{\beta}_1-\mu_1\varepsilon_1)<0. \tag{3.14}$$

However, the condition $\mathcal{R}_{0i}>1$ implies $\hat{\beta}_i\Lambda_j\hat{a}_j>\varepsilon_i\mu_i\hat{a}_j$, $i=1,2$ and $j\neq i$. Thus, the quantities $\Lambda_1\hat{\beta}_2-\mu_2\varepsilon_2$ and $\Lambda_2\hat{\beta}_1-\mu_1\varepsilon_1$ are positive, contradicting the inequality (3.14). □

Let us now investigate the existence and local stability of a generic co-endemic equilibrium, denoted by $\bar{E}=(\bar{S}_1,\bar{I}_1,\bar{S}_2,\bar{I}_2)$, where $\bar{I}_i>0$ for $i=1,2$. This equilibrium corresponds to a steady state in which the infection persists endemically in both patches. Due to the complexity of the model, it is not easy to establish the existence and the number of such equilibria. Some information regarding the existence and local stability of $\bar{E}$ can be obtained by employing the Castillo-Chavez and Song bifurcation theorem [14].

Theorem 3.3. *Assume that $\mathcal{R}_{0i}>1, i=1,2$ and $\mathcal{P}_1>1$. The equilibrium E_1 undergoes a transcritical forward bifurcation at $\mathcal{P}_2=1$: When $\mathcal{P}_2<1$, the equilibrium E_1 is locally asymptotically stable; when $\mathcal{P}_2>1$, E_1 becomes unstable and a locally stable co-endemic equilibrium $\bar{E}$ appears.*

Proof. We perform a bifurcation analysis on the equilibrium E_1, choosing $\hat{\beta}_2$ as bifurcation parameter and denoting by $\hat{\beta}_2^{\text{thr}}$ its value at the bifurcation point where $\mathcal{P}_2=1$, i.e.

$$\hat{\beta}_2^{\text{thr}}=\frac{\varepsilon_2}{S_2^*}. \tag{3.15}$$

To apply [14, Theorem 4.1], we compute the Jacobian matrix $J(E_1)$ at the bifurcation value $\hat{\beta}_2^{\text{thr}}$

$$J(E_1,\hat{\beta}_2^{\text{thr}})=\begin{bmatrix} -(\mu_1+a_1^*+d_3) & -(\varepsilon_1+d_1-d_4) & a_2^* & d_2\\ d_3 & -d_4 & 0 & 0\\ a_1^* & d_1 & -(\mu_2+a_2^*) & -(\varepsilon_2+d_2)\\ 0 & 0 & 0 & 0\end{bmatrix}.$$

The matrix $J(E_1,\hat{\beta}_2^{\text{thr}})$ has one simple zero eigenvalue and all the other eigenvalues with negative real parts. The left eigenvector v corresponding to the zero eigenvalue is $v=(0,0,0,1)$. Furthermore, since the right eigenvector $w=(w_1,w_2,w_3,w_4)$ has to satisfy the

condition $v\cdot w=1$, we get $w_4=1$. The other components of w are computed by solving the following linear system:

$$\begin{cases} (\mu_1+a_1^*+d_3)w_1+(\varepsilon_1+d_1-d_4)w_2-a_2^*w_3=d_2, & \text{(3.16a)}\\ -d_3w_1+d_4w_2=0, & \text{(3.16b)}\\ -a_1^*w_1-d_1w_2+(\mu_2+a_2^*)w_3=-(\varepsilon_2+d_2).[0.5ex] & \text{(3.16c)} \end{cases}$$

From (3.16b), we derive that

$$w_1=\frac{d_4}{d_3}w_2. \tag{3.17}$$

Substituting Eq. (3.17) in (3.16a) yields

$$w_3=\left[\frac{(\mu_1+a_1^*)d_4+(\varepsilon_1+d_1)d_3}{a_2^*d_3}\right]w_2-\frac{d_2}{a_2^*}. \tag{3.18}$$

We substitute expressions (3.17) and (3.18) in Eq. (3.16c) to obtain w_2. After some computations, we get

$$w_2=\frac{(\mu_2d_2-\varepsilon_2a_2^*)d_3}{d_4(\mu_1\mu_2+\mu_1a_2^*+\mu_2a_1^*)+d_3(\varepsilon_1\mu_2+\varepsilon_1a_2^*+\mu_2d_1)}. \tag{3.19}$$

Combining Eq. (3.18) and Eq. (3.19) yields the explicit expression of w_3

$$w_3=-\frac{d_4(\mu_1d_2+\varepsilon_2\mu_1+\varepsilon_2a_1^*)+d_3(\varepsilon_1\varepsilon_2+d_1\varepsilon_2+d_2\varepsilon_1)}{d_4(\mu_1\mu_2+\mu_1a_2^*+\mu_2a_1^*)+d_3(\varepsilon_1\mu_2+\varepsilon_1a_2^*+\mu_2d_1)}<0. \tag{3.20}$$

Note that $w_4\geq 0$, as required by [14, Remark 1].

The direction of the bifurcation at $\mathcal{P}_2=1$ is determined by the sign of the coefficients $\mathcal{A}$ and $\mathcal{B}$, where

$$\begin{aligned}\mathcal{A}&=\sum_{i,j=1}^{6}w_iw_j\frac{\partial^2 f_4}{\partial x_i\partial x_j}(E_1,\hat{\beta}_2^{\text{thr}})=2\frac{\partial^2 f_4(E_1)}{\partial S_2\partial I_2}w_3+\frac{\partial^2 f_4(E_1)}{\partial I_2\partial I_2}\\&=2\left[\frac{\varepsilon_2}{S_2^*}w_3+\beta_2'(0)g_2'(0)S_2^*\right]<0,\end{aligned}$$

since $\beta_2'(0)g_2'(0)S_2^*<0$ and $w_3<0$, and

$$\mathcal{B}=\sum_{i=1}^{4}w_i\frac{\partial^2 f_4}{\partial x_i\partial\hat{\beta}_2}\left(E_1,\hat{\beta}_2^{\text{thr}}\right)=\frac{\partial^2 f_4}{\partial I_2\partial\hat{\beta}_2}\left(E_1,\hat{\beta}_2^{\text{thr}}\right)=\frac{\partial\beta_2}{\partial\hat{\beta}_2}\big(g_2(0)\big)S_2^*>0.$$

Therefore, $\mathcal{A}<0$ and $\mathcal{B}>0$ and the equilibrium E_1 undergoes a transcritical forward bifurcation at $\mathcal{P}_2=1$. □

An analogous result holds for the equilibrium E_2.

Theorem 3.4. *Assume that $\mathcal{R}_{0i}>1, i=1,2$ and $\mathcal{P}_2>1$. The equilibrium E_2 undergoes a transcritical forward bifurcation at $\mathcal{P}_1=1$: When $\mathcal{P}_1<1$, the equilibrium E_2 is locally asymptotically stable; when $\mathcal{P}_1>1$, E_2 becomes unstable and a locally stable co-endemic equilibrium $\bar{E}$ appears.*

The following corollary is a direct consequence of Theorems 3.3 and 3.4.

Corollary 3.1. *Let $\mathcal{R}_{0i}>1, i=1,2$. If $\mathcal{P}_1>1$ and $\mathcal{P}_2>1$, there exists at least one co-endemic equilibrium $\bar{E}$ and it is locally asymptotically stable.*

4 Memory-dependent awareness

4.1 A variant of model (2.6)

In some cases, it is suitable to assume that the behaviour of individuals may depend not only on the current prevalence of the epidemic, but also on its past history [40, 54]. Such an assumption requires a variant of model (2.6) where the awareness variable $m_i(t)$ must take into account the memory effects. Following [34, 43, 59], the balance equation of the awareness variable is given by

$$\dot{m}_i(t)=c_i\big(g_i(I_i)-m_i\big), \quad i=1,2, \tag{4.1}$$

where the function g_i is the same function defined in Section 2.1, and it is assumed that the memory of individuals decays exponentially. Therefore, c_i is the inverse of the characteristic memory length and can be interpreted as the average time delay in the collection of information of the disease [54].

The "extended" model is governed by the following system of non-linear ordinary differential equations:

$$\dot{S}_1(t)=\Lambda_1-\mu_1 S_1-\beta_1(m_1)S_1I_1-a_1(m_1,m_2)S_1+a_2(m_1,m_2)S_2, \tag{4.2a}$$
$$\dot{I}_1(t)=\beta_1(m_1)S_1I_1-\varepsilon_1 I_1, \tag{4.2b}$$
$$\dot{m}_1(t)=c_1\big(g_1(I_1)-m_1\big), \tag{4.2c}$$
$$\dot{S}_2(t)=\Lambda_2-\mu_2 S_2-\beta_2(m_2)S_2I_2+a_1(m_1,m_2)S_1-a_2(m_1,m_2)S_2, \tag{4.2d}$$
$$\dot{I}_2(t)=\beta_2(m_2)S_2I_2-\varepsilon_2 I_2, \tag{4.2e}$$
$$\dot{m}_2(t)=c_2\big(g_2(I_2)-m_2\big) \tag{4.2f}$$

with initial conditions

$$S_i(0)>0, \quad I_i(0)\geq 0, \quad m_i(0)\geq 0. \tag{4.3}$$

Remark 4.1. In Remark 2.1, we observed that the awareness variable $m_i(t)$ in model (2.6) can be interpreted as a special case of the more general concept of information index, by choosing the Dirac delta function as memory kernel. Analogously, the memory-dependent awareness variable governed by the differential equation (4.1) can also be derived from the distributed delay equation (2.2). Indeed, by setting $g_i(t)=g_i(I_i(t))$ and $\rho_i(t)=c_ie^{-c_it}$ in (4.1), we obtain Eq. (4.1) by applying the so-called linear chain trick [39].

4.2 Equilibria and stability properties

We begin by noting that the existence and location of the disease-free equilibrium E_0, as well as the mixed equilibria E_1 and E_2, are the same as those obtained in Section 3. In fact, at any equilibrium $(\bar{S}_1,\bar{I}_1,\bar{m}_1,\bar{S}_2,\bar{I}_2,\bar{m}_2)$ of model (4.2), the awareness variables satisfy

$$\bar{m}_i = g_i(\bar{I}_i), \quad i=1,2.$$

Therefore, the equilibria of model (4.2) coincide with those of model (2.6), and the parameters c_1 and c_2 do not influence either their existence or their coordinates. In addition, we also point out that the form of the awareness variables does not even affect the computation of the basic reproduction number $\mathcal{R}_0$ nor the local stability of the disease-free steady state, since the computation of $\mathcal{R}_0$ requires the evaluation of the transition and transmission matrices at the disease-free steady state, where $I_i=0, i=1,2$. In this case, both travel and transmission rates are constant, and the model reduces to the one studied in Yang, Wu, Li and Ma [58]. Finally, as already noted in Remark 3.1, the stability properties of the disease-free equilibrium stated in Proposition 3.3 and Theorem 3.1 continue to hold also in the case of memory-dependent awareness.

In what follows, we perform the local stability analysis of the mixed equilibria. The analysis will be performed for the equilibrium $E_1=(S_1^*,I_1^*,0,S_2^*)$ in which the disease is endemic only in patch-1. Analogously, we can use the same argument for the equilibrium $E_2=(S_1^{**},0,I_2^{**},S_2^{**})$. Preliminarily, we introduce some quantities which will be useful in the forthcoming analysis. Let us set

$$g_1'=g_1'(I_1^*), \quad s=\mu_1+\mu_2+a_1^*+a_2^*, \quad p=\mu_1\mu_2+\mu_1 a_2^*+\mu_2 a_1^*, \tag{4.4}$$

and

$$\begin{aligned} &l_2=s+g_1'd_4+d_3, && q_1=d_3+s,\\ &l_3=g_1'd_4s+d_3(\mu_2+a_2^*+\varepsilon_1)+g_1'd_1d_3, && q_2=p+d_3(\mu_2+a_2^*+\varepsilon_1),\\ &l_4=g_1'd_4p+\mu_2g_1'd_1d_3+\varepsilon_1d_3(\mu_2+a_2^*), && q_3=\varepsilon_1d_3(\mu_2+a_2^*), \end{aligned} \tag{4.5}$$

where $d_i, i=1,\dots,4$, are the positive quantities defined in (3.10).

Furthermore, let us set

$$\begin{aligned} &\xi_1=l_2l_3-l_4, && \xi_3=q_1q_2l_3+q_2q_3+q_1q_3l_2-2l_2q_3-q_1^2l_4,\\ &\xi_2=q_2l_3+q_1l_2l_3+q_3l_2-l_3^2-2q_1l_4, && \xi_4=q_1q_2q_3-q_3^2. \end{aligned} \tag{4.6}$$

It is not hard to check that the quantities ξ_1 and ξ_4 are strictly positive for all parameter values. Indeed, observing that $s^2>p$ yields

$$\begin{aligned} l_2l_3 &> sl_3 = g_1'd_4s^2+d_3(\mu_2+a_2^*+\varepsilon_1)s+g_1'd_1d_3s\\ &> g_1'd_4s^2+d_3\varepsilon_1s+g_1'd_1d_3s > g_1'd_4p+d_3\varepsilon_1(\mu_2+a_2^*)+g_1'd_1d_3\mu_2 = l_4, \end{aligned}$$

that is, $\xi_1>0$. Analogously, we get

$$\begin{aligned} q_1q_2 &> sl_3=(d_3+s)[p+d_3(\mu_2+a_2^*+\varepsilon_1)]>sd_3(\mu_2+a_2^*+\varepsilon_1)\\ &> sd_3\varepsilon_1>(\mu_2+a_2^*)d_3\varepsilon_1=q_3, \end{aligned}$$

hence $\xi_4>0$.

The following result can be established.

Theorem 4.1. *Let $\mathcal{R}_{01}>1$. If $\mathcal{P}_2>1$, then the endemic equilibrium E_1 is unstable. If $\mathcal{P}_2<1$, then the local stability of E_1 is governed by the number of positive real roots of the cubic polynomial*

$$f(c_1)=\xi_1c_1^3+\xi_2c_1^2+\xi_3c_1+\xi_4.$$

Specifically, the following scenarios may arise:

- *(i) If the polynomial $f(c_1)$ admits no positive real roots, then E_1 is locally asymptotically stable for all $c_1>0$.*
- *(ii) If the polynomial $f(c_1)$ admits a single positive real root $\overline{c}_1$ of multiplicity two, then E_1 is locally asymptotically stable for all $c_1>0$, except at $c_1=\overline{c}_1$, where it loses hyperbolicity.*
- *(iii) If the polynomial $f(c_1)$ admits two simple positive roots $\overline{c}_1<\tilde{c}_1$, then E_1 is locally asymptotically stable for $c_1\in(0,\overline{c}_1)\cup(\tilde{c}_1,+\infty)$, and unstable for $c_1\in(\overline{c}_1,\tilde{c}_1)$. A Hopf bifurcation occurs at each of the critical values $c_1=\overline{c}_1$ and $c_1=\tilde{c}_1$.*

Proof. By linearising system (4.2) at the equilibrium E_1, we get the characteristic equation $\det(\lambda\mathrm{I}-J(E_1))=0$, i.e.

$$\begin{vmatrix} \lambda+\mu_1+a_1^*+d_3 & \varepsilon_1 & d_1-d_4 & -a_2^* & 0 & -d_2\\ -d_3 & \lambda & d_4 & 0 & 0 & 0\\ 0 & -c_1g_1' & \lambda+c_1 & 0 & 0 & 0\\ -a_1^* & 0 & -d_1 & \lambda+\mu_2+a_2^* & \hat{\beta}_2S_2^* & d_2\\ 0 & 0 & 0 & 0 & \lambda+\varepsilon_2-\hat{\beta}_2S_2^* & 0\\ 0 & 0 & 0 & 0 & -c_2g_2'(0) & \lambda+c_2 \end{vmatrix}=0.$$

Two roots of the characteristic equation are $\lambda_5=\mathcal{P}_2-1$ and $\lambda_6=-c_2$. Hence, a necessary condition to have the local asymptotic stability of E_1 is $\mathcal{P}_2<1$.

Removing the fifth and sixth rows and columns and adding the second and fourth rows to the first one leads to

$$\begin{vmatrix} \mu_1+\lambda & +\varepsilon_1+\lambda & 0 & +\mu_2+\lambda\\ -d_3 & \lambda & d_4 & 0\\ 0 & -c_1g_1' & \lambda+c_1 & 0\\ -a_1^* & 0 & -d_1 & \lambda+\mu_2+a_2^* \end{vmatrix}=0,$$

that is,

$$P(\lambda)=\lambda^4+\mathcal{A}_1\lambda^3+\mathcal{A}_2\lambda^2+\mathcal{A}_3\lambda+\mathcal{A}_4=0,$$

where

$$\begin{aligned}\mathcal{A}_1&=c_1+q_1, \qquad \mathcal{A}_2=l_2c_1+q_2,\\ \mathcal{A}_3&=l_3c_1+q_3, \quad \mathcal{A}_4=l_4c_1,\end{aligned}$$

and the coefficients l_i, $q_i, i=1,\dots 4$ are defined in (4.5).

Routh-Hurwitz criterion states that all roots of the characteristic equation have negative real parts if and only if all the Hurwitz determinant are positive, that is:

(i) $\mathcal{A}_i>0, i=1,\dots,4$,
(ii) $\mathcal{A}_1\mathcal{A}_2\mathcal{A}_3-\mathcal{A}_3^2-\mathcal{A}_1^2\mathcal{A}_4>0$.

Condition (i) is clearly satisfied for all the parameter values. To determine conditions under which the third-order Hurwitz determinant is positive, we express the coefficients $\mathcal{A}_i$ as functions of the parameter c_1. We choose c_1 as a bifurcation parameter since it does not affect the existence or the coordinates of the equilibrium E_1. Rewriting the inequality (ii) depending on c_1 leads to

$$f(c_1)=\mathcal{A}_1(c_1)\mathcal{A}_2(c_1)\mathcal{A}_3(c_1)-\mathcal{A}_3^2(c_1)-\mathcal{A}_1^2(c_1)\mathcal{A}_4(c_1)>0, \tag{4.7}$$

that is,

$$f(c_1)=\xi_1c_1^3+\xi_2c_1^2+\xi_3c_1+\xi_4>0,$$

where the coefficients $\xi_i, i=1,\dots,4$, are given in (4.6).

As observed previously, the coefficients ξ_1 and ξ_4 are positive. Then, the number of sign changes in the sequence of coefficients of the polynomial $f(c_1)$ can be either 0 or 2. If the intermediate coefficients ξ_2 and ξ_3 are also positive, then $f(c_1)>0$ for all $c_1>0$, and the equilibrium E_1 is locally asymptotically stable. Conversely, two sign changes occur if ξ_1 or ξ_4 are negative, indicating the possibility of instability.

In this case, Descartes' rule of signs ensures that the number of positive real roots of the polynomial $f(c_1)$, counted with multiplicity, can be either 0 or 2. If $f(c_1)$ does not have positive real roots, we have that $f(c_1)>0$ for every $c_1>0$. Hence, the third-order Hurwitz determinant is positive and the equilibrium E_1 is locally asymptotically stable for all $c_1>0$.

If $f(c_1)$ has a single positive real root $\overline{c}_1$ of multiplicity two, then E_1 is locally asymptotically stable for all $c_1>0$, except at $c_1=\overline{c}_1$, where the third-order Hurwitz determinant vanishes.

Finally, if that the polynomial $f(c_1)$ admits two positive real roots $\overline{c}_1<\tilde{c}_1$, equilibrium E_1 is unstable for $c_1\in(\overline{c}_1,\tilde{c}_1)$, and locally asymptotically stable for $c_1\notin(\overline{c}_1,\tilde{c}_1)$. Furthermore, since both the roots are simple, it follows that $f'(\overline{c}_1)\neq 0$ and $f'(\tilde{c}_1)\neq 0$. Therefore, the non–zero speed condition is satisfied [30, Corollary 3.3], and the equilibrium E_1 undergoes a Hopf bifurcation at $\overline{c}_1$ and $\tilde{c}_1$. □

Remark 4.2. Theorem 4.1 states that the necessary conditions for the occurrence of a Hopf bifurcation are $\xi_2 < 0$ and $\xi_3 < 0$, where the coefficients ξ_2 and ξ_3 are defined in (4.6). The sign of these coefficients depends on the functional forms of the awareness-dependent parts of the contact and travel rates. In fact, both ξ_2 and ξ_3 contain the terms d_1 and d_4 defined in Eq. (4.5), which, in turn, include the derivatives of the contact and travel rates with respect to the awareness variable m_1. Therefore, the possible occurrence of a Hopf bifurcation is intrinsically linked to how individuals modify their contact and mobility behaviours in response to perceived infection risk.

5 Numerical simulations

5.1 Functional forms of the awareness variables and awareness-dependent rates

In order to perform the numerical simulations, we need to select the functional forms of the functions g_i, c_i^F and a_i, introduced in (2.1), (2.3) and (2.5).

i) Awareness variables. We assume that the function g_i is proportional to the disease prevalence I_i in the i-th patch

$$g_i(I_i) = k_i I_i, \quad i = 1,2. \tag{5.1}$$

The parameter $k_i \in (0,1]$ represents the information coverage regarding the epidemic status in patch-i. It can be interpreted as the "summary" of two contrasting phenomena: The disease under-reporting (here assumed to be the prevailing phenomenon) mainly due to technical reasons related to the screening procedures, and the overestimation of the cases usually induced by media and rumours on the disease status [40].

ii) Intra-patch contact rates. As discussed in Subsection 2.2, the function c_i^F is required to be increasing with respect to the awareness variable m_i, $c_i^F(0) = 0$ and $\sup c_i^F(m_i) < \hat{c}_i$. These conditions are satisfied by a Holling type II functional response

$$c_i^F(m_i) = \hat{c}_i \frac{\delta_i m_i}{1+\delta_i m_i}, \quad i = 1,2. \tag{5.2}$$

The positive constant $\delta_i, i = 1,2$, can be interpreted as a measure of how quickly the individuals of the i-th patch react to awareness and voluntarily reduce their contact patterns. This functional form has been employed in several behavioural epidemic models to represent the behavioural-dependent part of the contact rate [9, 12, 22]. With this choice, the awareness-dependent transmission rate assumes the form

$$\beta_i(m_i) = \frac{\hat{\beta}_i}{1+\delta_i m_i}, \qquad i = 1,2. \tag{5.3}$$

iii) Inter-patch travel rates. As introduced in Subsection 2.3, the travel rate a_i from patch-i to patch-j depends on the awareness variables through the function $z_i(m_1, m_2) =$

$\theta_i(m_i - m_j)$ with $\theta_i \in [0,1]$. The function $a_i(z_i)$ is assumed to satisfy the following conditions: (i) $a_i(0) = \hat{a}_i$, where $\hat{a}_i$ is the travel rate from patch-i in absence of epidemics; (ii) a_i is increasing with respect to z_i; (iii) $a_i(z_i)$ is nonnegative in its domain.

A suitable choice satisfying these requirements is

$$a_i(z_i) = \hat{a}_i \left(1 + \frac{z_i}{g_j(\bar{N})}\right), \quad i = 1,2, \quad j \neq i, \tag{5.4}$$

where

$$\bar{N} = \frac{\Lambda_1 + \Lambda_2}{\min\{\mu_1, \mu_2\}}.$$

In fact, since $m_i(t) \leq g_i(\bar{N})$ for $t \geq 0$, it trivially follows that $-g_j(\bar{N}) \leq z_i \leq g_i(\bar{N})$, and thus $a_i(z_i)$ remains nonnegative for all admissible values of z_i.

5.2 Parameter values and initial conditions

Here, we perform some numerical simulations to illustrate the qualitative behaviour of the model and to support the discussion of the analytical results. The parameter values used here, which are purely theoretical and not associated with any specific case study, are reported in Table 1.

Table 1: Parameter values of model (2.6) used for the numerical simulations. All parameter values are theoretical and chosen for illustrative purposes. The recruitment rates Λ_i, natural death rates μ_i, and recovery rates γ_i are consistent with those used in [36], while the remaining parameters are assumed.

Parameter	Value	Description
Λ_1	1000	Recruitment rate in patch-1
Λ_2	200	Recruitment rate in patch-1
μ_1	0.001	Natural death and emigration rate in patch-1
μ_2	0.002	Natural death and emigration rate in patch-2
d_1	$6 \cdot 10^{-7}$	Disease-induced death rate in patch-1
d_2	$1 \cdot 10^{-6}$	Disease-induced death rate in patch-2
γ_1	0.8	Recovery rate in patch-1
γ_2	0.5	Recovery rate in patch-2
$\hat{a}_1$	0.5	Baseline travel rate from patch-1
$\hat{a}_2$	0.6	Baseline travel rate from patch-2
$\hat{\beta}_1$	$7 \cdot 10^{-6}$	Baseline transmission rate in patch-1
$\hat{\beta}_2$	$5 \cdot 10^{-6}$	Baseline transmission rate in patch-2
k_1	0.7	Information coverage in patch-1
k_2	0.4	Information coverage in patch-2
δ_1	0.005	Reactivity of patch-1 population to reduce interpersonal contacts
δ_2	0.003	Reactivity of patch-2 population to reduce interpersonal contacts
θ_1	0.2	Mobility responsiveness parameter in patch-1
θ_2	0.5	Mobility responsiveness parameter in patch-2

To explore the role of heterogeneity between regions, we assign slightly different parameter values to the two patches. As highlighted in [47], assuming identical parameters across patches can reduce or even hide the impact of spatial dispersal on the epidemic dynamics. In this framework, patch-1 is intended to represent a more developed country or urban area, characterised by a higher recruitment rate, longer life expectancy, and greater attractiveness in terms of mobility. Conversely, patch-2 represents a less developed environment, characterised by a lower recruitment rate and a shorter average lifespan.

The values of the recruitment rates Λ_i, natural death rates μ_i, recovery rates γ_i, and baseline travel rates $\hat{a}_i, i=1,2$, are those employed in the theoretical study [36], while the remaining parameters are assumed. In particular, we consider a higher disease-induced mortality rate d_2 in patch-2 and a higher baseline transmission rate $\hat{\beta}_1$ in patch-1. This choice reflects the assumption of a higher per capita contact rate in patch-1, which represents a more developed and urbanised area where individuals are more likely to have frequent interactions due to work or social activities. On the other hand, the higher disease-induced mortality rate in patch-2 is consistent with the interpretation of this patch as a less developed environment, with limited access to healthcare services.

The information coverages k_1 and k_2 are chosen to reflect better-quality information in patch-1, with $k_1 = 0.7$ and $k_2 = 0.4$. Although assumed, these values are consistent with those reported in the literature, where behavioural models have been calibrated to real-world case studies [9, 10].

The reactivity parameter δ_1 is chosen higher than δ_2, consistent with the interpretation of patch-1 as a more developed setting. By contrast, the parameter θ_1, expressing the degree to which awareness influences the travel rate from patch-1, is taken to be lower than θ_2. The purpose of this choice is to reflect the situation in which individuals from the more developed region may be less inclined or able to change their travel behaviour toward the less developed region, as their movements are more likely to be driven by essential needs, such as work or family. Therefore, individuals may not be able to change their travel patterns even when they are aware of an increased epidemic risk.

Finally, we set the initial conditions as $N_i(0)=10^5, I_i(0)=10^3, R_i(0)=0, i=1,2$.

5.3 Effects of awareness-induced behavioural changes on the stability of mixed equilibria

In Remark 3.2, we observed that, for suitable parameter values, the mixed equilibria may be stable in the unresponsive scenario and lose stability in the responsive scenario, where individuals adjust their contact and mobility patterns in response to awareness. In this section, we numerically explore and compare the solutions of model (2.6) obtained in both the unresponsive and responsive scenarios.

The parameters used to simulate the responsive scenario are those reported in Table 1. In particular, the baseline transmission rates $\hat{\beta}_1$ and $\hat{\beta}_2$ have been chosen such that the corresponding basic reproduction numbers, $\mathcal{R}_{01}$ and $\mathcal{R}_{02}$, are of on the order of magnitude of one but still greater than one, to ensure the existence of both mixed equilibria.

Specifically, we set $\hat{\beta}_1 = 7 \cdot 10^{-6}$ and $\hat{\beta}_2 = 5 \cdot 10^{-6}$, which yield $\mathcal{R}_{01} = 3.94$ and $\mathcal{R}_{02} = 3.73$. The responsiveness parameters δ_i and θ_i, for $i = 1,2$, have been set so that the resulting values of $\mathcal{P}_1$ and $\mathcal{P}_2$ are of order one. This choice is due to the epidemiological interpretation of $\mathcal{P}_i, i = 1,2$, as the average number of secondary infections produced by an infectious individual residing in patch-i, when the disease is at the endemic steady state in the other patch.

The unresponsive scenario, in which individuals do not adjust their contact and travel pattern in response to awareness, is obtained by setting all the parameter values as in Table 1, except for the reactivity parameters δ_i and θ_i, for $i = 1,2$, both set equal to 0. Therefore, the travel rates $a_i(m_1, m_2)$ and transmission rates $\beta_i(m_i)$ remain constantly equal to their respective baseline values, $\hat{a}_i$ and $\hat{\beta}_i$.

The simulations, carried out using the MATLAB solver `ode45`, are presented in Fig. 2. In the unresponsive scenario (panel (a)), the reproduction numbers $\hat{\mathcal{P}}_1 = 1.07$ and $\hat{\mathcal{P}}_2 = 0.95$, indicate that the mixed equilibrium E_1 is locally asymptotically stable. In contrast, in the responsive scenario (panel (b)), the reproduction numbers increase to $\mathcal{P}_1 = 2.04$ and $\mathcal{P}_2 = 2.15$, resulting in the stability of the co-endemic equilibrium $\bar{E}$.

In addition, the I_1-coordinate of the equilibrium E_1 in the unresponsive scenario is $I_1^* = 1117$ individuals. When individuals respond to awareness by modifying their contact and travel behaviour, the coordinates of the co-endemic equilibrium become approximately $\bar{I}_1 = 282$ and $\bar{I}_2 = 733$ infected individuals. This suggests that, at equilibrium, the total number of infected individuals decreases when passing from the unresponsive to the responsive scenario. However, in the responsive case, there are more infected indi-

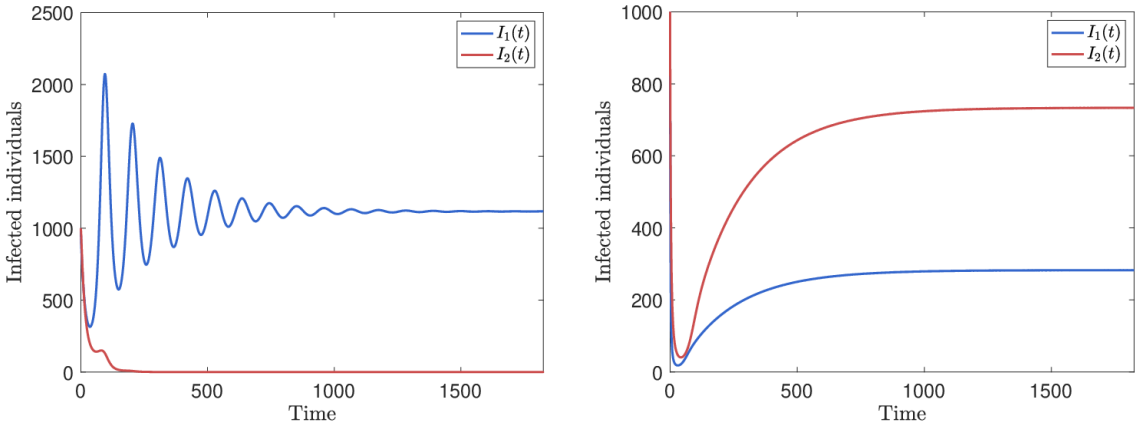

(a) unresponsive scenario (b) responsive scenario

Figure 2: Effects of awareness-induced behavioural changes on the stability of mixed equilibria of model (2.6). Panel (a) illustrates the unresponsive scenario, where the population does not modify its behaviour. This scenario is obtained by setting $\delta_i = \theta_i = 0$ and the remaining parameter as in Table 1. In this case, we have $\hat{\mathcal{P}}_1 = 1.07$ and $\hat{\mathcal{P}}_2 = 0.95$, implying that equilibrium E_1 is locally asymptotically stable. Panel (b) shows the responsive scenario, obtained by setting all the parameter values as in Table 1. Here, $\mathcal{P}_1 = 2.04$ and $\mathcal{P}_2 = 2.15$, leading to the stability of the co-endemic equilibrium.

viduals in patch-2 than in patch-1. This asymmetry appears to be driven by the lower value of the reactivity parameter δ_2, which indicates a lower behavioural response in patch-2. In fact, additional simulations (not shown here) reveal that increasing the value of the parameter δ_2 leads to a reduction in the value of $\bar{I}_2$.

5.4 Effects of awareness-induced behavioural changes on the epidemic burden

We evaluate the impact of both the reactivity parameter δ_1 and the mobility responsiveness parameter θ_1 on the basic reproduction number $\mathcal{P}_2$, whose threshold determines the stability of the equilibrium E_1. To this aim, we perform the contour plot of the basic reproduction number $\mathcal{P}_2$ as a function of both δ_1 and θ_1.

As shown in Fig. 3, $\mathcal{P}_2$ depends almost exclusively on the reactivity parameter δ_1, as can be deduced by the almost vertical contour lines. In contrast, $\mathcal{P}_2$ is only weakly sensitive to changes in θ_1. This behaviour arises from the specific functional forms chosen for the intra-patch contact rates and the inter-patch travel rates.

Indeed, by substituting the functional forms of the contact and mobility rates given in Eqs. (5.3) and (5.4) into the expression for $\mathcal{P}_2$ given in Eq. (3.9), one can observe that $\mathcal{P}_2$ depends linearly on both the reactivity parameters δ_1 and θ_1. However, the contribution of θ_1 is scaled by the factor $k_2\bar{N}$, where $\bar{N} = (\Lambda_1+\Lambda_2)/\min\{\mu_1,\mu_2\}$ is the upper bound of the total population size. This scaling significantly reduces the sensitivity of $\mathcal{P}_2$ to variations in θ_1 compared to δ_1.

We analyse the impact of the parameters δ_1 and θ_1 on the overall disease burden, by considering two relevant quantities: (i) the total cumulative incidence $\mathrm{CI}(t)$, i.e. the total number of new cases observed in both patches in the time interval $[0,t]$; and (ii) the

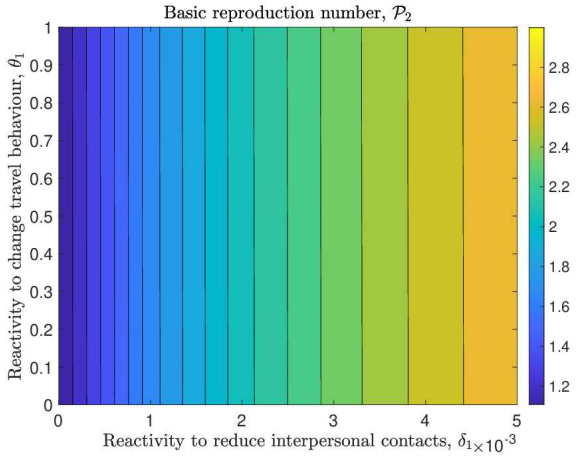

Figure 3: Contour plot of the reproduction number $\mathcal{P}_2$ as a function of the parameters δ_1 and θ_1, representing the responsiveness of patch-1 to reduce interpersonal contacts and to change mobility behaviours, respectively. The values of the parameters are reported in Table 1.

total cumulative disease-induced deaths $\mathrm{CD}(t)$, i.e. the total number of deaths due to the disease in both patches in the time interval $[0,t]$. These quantities can be expressed as follows:

$$\mathrm{CI}(t) = \int_0^t \left[\beta_1\big(m_1(\tau)\big)S_1(\tau)I_1(\tau) + \beta_2\big(m_2(\tau)\big)S_2(\tau)I_2(\tau)\right]d\tau,$$
$$\mathrm{CD}(t) = \int_0^t \left[d_1 I_1(\tau) + d_2 I_2(\tau)\right]d\tau.$$

For illustrative purposes, we perform contour plots of $\mathrm{CI}(\bar{t})$ and $\mathrm{CD}(\bar{t})$ as functions of the parameters δ_1 and θ_1, where $\bar{t} = 2000$. The almost vertical contour lines in Fig. 4 indicate that the aforementioned quantities depend almost exclusively on the parameter δ_1, which represents the reactivity of individuals living in patch-1 to reduce their interpersonal contacts.

Fig. 4 also highlights a seemingly counter-intuitive pattern: the cumulative total incidence $\mathrm{CI}(\bar{t})$ decreases monotonically with δ_1, while the cumulative deaths $\mathrm{CD}(\bar{t})$ increase with δ_1, reaching their maximum when $\delta_1 = 0.005$. This result stems from the influence of δ_1 and θ_1 on the reproduction number $\mathcal{P}_2$. When $\delta_1 = 0$, the equilibrium E_1 is stable (see Fig. 2(a)), and the disease remains endemic in patch-1 only. Increasing the value of δ_1 leads to an increase in the basic reproduction number $\mathcal{P}_2$, which in turn leads to the stability of the co-endemic steady state by crossing the threshold value 1 (see Fig. 2(b)). Furthermore, additional simulations (not included here for the sake of brevity) suggest that the I_2-coordinate of the co-endemic equilibrium increases with δ_1. Since patch-2 is assumed to have a higher disease-induced mortality rate d_2, this leads to a larger number of cumulative deaths as δ_1 increases. Nevertheless, $\mathrm{CI}(\bar{t})$ decreases with δ_1, consistently with the lower total number of infected individuals at the co-endemic equilibrium, compared to the case in which the disease persists in one patch only.

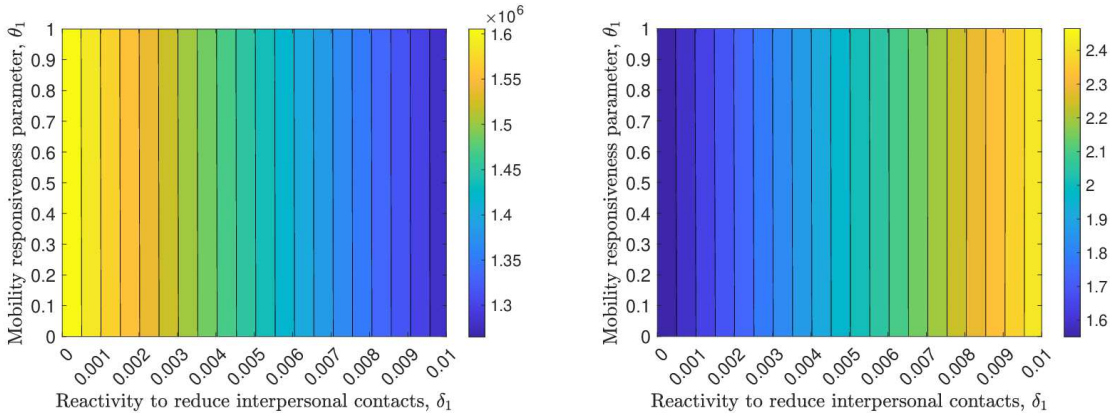

(a) $\mathrm{CI}(t)$ (b) $\mathrm{CD}(t)$

Figure 4: Contour plots of the total cumulative incidence $\mathrm{CI}(t)$ and total cumulative disease-induced deaths $\mathrm{CD}(t)$ at $\bar{t} = 2000$, versus the reactivity parameter δ_1 to reduce interpersonal contacts and versus the mobility responsiveness parameter θ_1 of patch-1. The values of the parameters are reported in Table 1.

6 Final remarks and future perspectives

In this work, we have proposed and analysed a two-patch behavioural SIR epidemic model in which individuals adjust their contact and mobility patterns in response to perceived infection risk. While previous studies have investigated the dynamics of patch models with prevalence-dependent contact or dispersal rates [47–49, 57], the joint influence of awareness on both contact and mobility patterns remains largely underexplored. To address this gap, we introduced two awareness variables that quantify the perceived risk of infection in each patch and affect both contact and travel rates.

We first extended the two-patch SIR model proposed in Yang, Wu, Li, and Ma [58] by defining two awareness variables $m_i(t), i = 1,2$, as functions of the current prevalence in the i-th patch, thereby assuming that behavioural response is based only on the current epidemic status. Then, we proposed a model formulation in which awareness incorporates memory of past epidemic values.

Through a qualitative analysis of the model based on stability and bifurcation theory, we derived threshold conditions for the existence and stability of the disease-free, mixed, and co-endemic equilibria. In particular, we obtained global stability conditions for the disease-free equilibrium under both constant and prevalence-dependent dispersal rates. The threshold stability conditions for mixed equilibria are derived in terms of the basic reproductive number $\mathcal{P}_i$ in the i-th patch, $i = 1,2$, when dispersal occurs between the patches and the other patch is at the endemic steady state. We derived sufficient conditions for the existence of a locally stable co-endemic equilibrium by proving the existence of a forward bifurcation when the minimum between the two reproduction numbers $\mathcal{P}_i$, $i = 1,2$, crosses the threshold value of 1.

Our analysis reveals that awareness-induced behavioural changes can destabilise mixed equilibria by increasing $\mathcal{P}_i$, thereby promoting the emergence of a stable co-endemic steady state. In the presence of memory-dependent awareness, the mixed equilibria may further destabilise through Hopf bifurcations, depending on the sign of some awareness-related parameters. Numerical simulations show that behavioural responses can significantly influence some relevant quantities, such as the basic reproduction numbers $\mathcal{P}_i$, the total cumulative incidence and disease-induced mortality.

Understanding the complex interplay between awareness-driven behavioural adaptations, human mobility, and epidemic spread remains a significant challenge, with several open questions yet to be addressed. Despite the insights provided by this study, some limitations should be acknowledged. First, the functional forms used to model awareness-dependent contact and travel rates were drawn from existing literature on behavioural epidemic models and spatially structured models with prevalence-dependent behaviours [9, 10, 22, 47, 48, 57]. However, there is still lack of substantial literature where such functions have been validated against real data (a very recent example is given in [11]). As a result, the simulations presented here should be regarded as qualitative explorations of the model's dynamics rather than quantitative predictions of real-world scenarios.

Furthermore, although the theoretical analysis in the case with memory-dependent awareness has revealed conditions under which mixed equilibria may lose stability via Hopf bifurcations, finding a set of parameter values for which the coefficients ξ_2 and ξ_3 are negative is still an open problem. However, our findings are aligned with results obtained via alternative modelling approaches. For instance, in [48], a two-patch SIR model with constant dispersal is studied. There, the transmission rates depend on delayed prevalence to represent both the effects of media–driven surveillance on disease transmission and the possibly delayed spread of information. It is shown that Hopf bifurcations of mixed equilibria can indeed occur when infected individuals do not travel between patches.

In conclusion, this work can be seen as a further step towards understanding the interplay between human mobility, behavioural responses, and epidemic dynamics. At the same time, the limitations outlined above offer opportunities for future research. A first direction may be to revise the formulation of awareness, replacing its dependence on prevalence with dependence on incidence. Indeed, some recent works suggest that linking the epidemic risk perception to infection prevalence may be sometimes inaccurate, since prevalence may be an unobserved quantity [23]. A second direction may involve testing alternative functional forms to describe behavioural reactivity and applying the model to real-world case studies, to evaluate which forms best match the empirical data.

Appendix A.

Proof of Lemma 3.1. Let us denote by $[0,\eta)$ the maximal interval of existence of the solution, with $0<\eta\leq+\infty$. Define

$$\mathcal{T}:=\{t \mid x_i(\tau)>0, i=1,\dots,4, \tau\in[0,t]\}. \tag{A.1}$$

The set $\mathcal{T}$ is nonempty as $0\in\mathcal{T}$. Therefore, we can consider $t_1=\sup\mathcal{T}$ and $t_1\in(0,\eta]$. We claim that $x_i(t_1)>0, i=1,\dots,4$. To show this, note that Eq. (2.6a) can be rewritten as

$$\dot{S}_1(t)=B(t)-A(t)S_1(t), \tag{A.2}$$

where

$$B(t):=\Lambda_1+a_2(t)S_2(t), \quad A(t):=\mu_1+a_1(t)+\beta_1(t)I_1(t).$$

Multiplying both sides by $\exp\int_0^t A(\tau)d\tau$, Eq. (A.2) becomes

$$\frac{d}{dt}\{S_1(t)e^{\int_0^t A(\tau)d\tau}\}=B(t)e^{\int_0^t A(\tau)d\tau}.$$

Integrating both sides from 0 to t_1, we obtain

$$S_1(t_1)e^{\int_0^{t_1} A(\tau)d\tau}-S_1(0)=\int_0^{t_1} B(s)e^{\int_0^s A(\tau)d\tau}ds,$$

and so

$$S_1(t_1) = S_1(0)e^{-\int_0^{t_1} A(\tau)d\tau} + e^{-\int_0^{t_1} A(\tau)d\tau} \int_0^{t_1} B(s)e^{\int_0^s A(\tau)d\tau} ds > 0,$$

since $S_1(0) > 0$ and $B(s) > 0, s \in [0, t_1)$. The same argument can be applied to show that $x_i(t_1) > 0$ for $i = 2, \ldots, 4$.

Now, we claim that $t_1 = \eta$ and therefore the solution is strictly positive, for every $t > 0$. Suppose by contradiction that $t_1 < \eta$. Due to continuity of the solution, there exists $t_2 > t_1$ such that $x_i(t) > 0$ on $[0, t_2], i = 1, \ldots, 4$. Then $t_2 \in \mathcal{T}$. This leads to a contradiction, as $t_1 = \sup \mathcal{T}$. □

Proof of Proposition 3.1. Since the closure of a positively invariant set is still positively invariant [2, Remark 16.3h], it follows from Lemma 3.1 that $\mathbb{R}^4_+$ is positively invariant.

Adding the equations of model (2.6), we obtain the following equation ruling the evolution of the total population $N(t)$:

$$\begin{aligned} \dot{N}(t) &= \Lambda_1 + \Lambda_2 - \mu_1 N_1(t) - \mu_2 N_2(t) - \varepsilon_1 I_1(t) - \varepsilon_2 I_2(t) \\ &\leq \Lambda_1 + \Lambda_2 - \min\{\mu_1, \mu_2\} N(t), \end{aligned} \tag{A.3}$$

thus

$$0 < N(t) \leq N(0)e^{-\min\{\mu_1,\mu_2\}t} + \frac{\Lambda_1 + \Lambda_2}{\min\{\mu_1, \mu_2\}} (1 - e^{-\min\{\mu_1,\mu_2\}t}), \quad \forall t \geq 0, \tag{A.4}$$

and then

$$\limsup_{t \to +\infty} N(t) \leq \frac{\Lambda_1 + \Lambda_2}{\min\{\mu_1, \mu_2\}}. \tag{A.5}$$

From (A.4), we get that if $N(0) \leq (\Lambda_1 + \Lambda_2)/\min\{\mu_1, \mu_2\}$, then $N(t) \leq (\Lambda_1 + \Lambda_2)/\min\{\mu_1, \mu_2\}$ for all $t \geq 0$. On the other hand, if $N(0) > (\Lambda_1 + \Lambda_2)/\min\{\mu_1, \mu_2\}$, the solution $N(t)$ will have as upper bound $(\Lambda_1 + \Lambda_2)/\min\{\mu_1, \mu_2\}$ for $t \to +\infty$, for Eq. (A.5). This means that even if $N(0) > (\Lambda_1 + \Lambda_2)/\min\{\mu_1, \mu_2\}$, the solution $N(t)$ will become smaller than $(\Lambda_1 + \Lambda_2)/\min\{\mu_1, \mu_2\}$ or will approach it asymptotically. Then, the set Ω is positively invariant and attractive for the solutions of model (2.6). Since the solution is confined in the compact set Ω, the maximal interval of existence of $x(t)$ is $[0, +\infty)$ and the solution exists globally for $t > 0$. □

Acknowledgments

We sincerely thank the editor and reviewers for their careful reading and insightful comments, which have greatly helped to improve our manuscript.

This work has been carried out under the auspices of the Italian National Group for Mathematical Physics (GNFM) of the National Institute for Advanced Mathematics (INdAM). The research was supported by the EU funding within the NextGenerationEU – MUR PNRR Extended Partnership initiative on Emerging Infectious Diseases (Project No. PE00000007, INF-ACT). B. Buonomo also acknowledges PRIN 2020 project (No. 2020JLWP23) "Integrated Mathematical Approaches to Socio-Epidemiological Dynamics".

References

[1] L. J. Allen, F. Brauer, P. Van den Driessche, and J. Wu, *Mathematical Epidemiology*, in: Lecture Notes in Mathematics, Vol. 1945, Springer, 2008.

[2] H. Amann, *Ordinary Differential Equations: An Introduction to Nonlinear Analysis*, in: De Gruyter Studies in Mathematics, Vol. 13, De Gruyter, 2011.

[3] J. Arino, *Diseases in metapopulations*, in: Series in Contemporary Applied Mathematics, Vol. 11, Modeling and Dynamics of Infectious Diseases, World Scientific, 64–122, 2009.

[4] J. Arino, *Spatio-temporal spread of infectious pathogens of humans*, Infect. Dis. Model., 2:218–228, 2017.

[5] J. Arino, J. R. Davis, D. Hartley, R. Jordan, J. M. Miller, and P. van den Driessche, *A multi-species epidemic model with spatial dynamics*, Math. Med. Biol., 22:129–142, 2005.

[6] J. Arino and P. van den Driessche, *A multi-city epidemic model*, Math. Popul. Stud., 10:175–193, 2003.

[7] J. Arino and P. Van den Driessche, *Disease spread in metapopulations*, Fields Inst. Commun., 48:1–13, 2006.

[8] F. Brauer, P. Van den Driessche, and L. Wang, *Oscillations in a patchy environment disease model*, Math. Biosci., 215(1):1–10, 2008.

[9] B. Buonomo and R. Della Marca, *Effects of information-induced behavioural changes during the COVID-19 lockdowns: The case of Italy*, R. Soc. Open Sci., 7:201635, 2020.

[10] B. Buonomo and R. Della Marca, *A behavioural vaccination model with application to meningitis spread in Nigeria*, Appl. Math. Model., 125:334–350, 2024.

[11] B. Buonomo, R. Della Marca, and M. D. Asfaw, *Modelling human response to information in voluntary vaccination behaviour using epidemic data*, Math. Biosci. Eng., 22:1185–1205, 2025.

[12] B. Buonomo, R. Della Marca, and S. S. Sharbayta, *A behavioral change model to assess vaccination-induced relaxation of social distancing during an epidemic*, J. Biol. Syst., 30(1):1–25, 2022.

[13] B. Buonomo, A. d'Onofrio, and D. Lacitignola, *Global stability of an SIR epidemic model with information dependent vaccination*, Math. Biosci., 216:9–16, 2008.

[14] C. Castillo-Chavez and B. Song, *Dynamical models of tuberculosis and their applications*, Math. Biosci. Eng., 1:361–404, 2004.

[15] C. Castillo-Chavez and H. Thieme, *Asymptotically Autonomous Epidemic Models*, Biometrics Unit Technical Reports, BU-1248-M, Cornell University, 1994. `https://ecommons.cornell.edu/server/api/core/bitstreams/a05d3117-5e56-4d77-9220-681b913b10ff/content`

[16] M. Chinazzi et al., *The effect of travel restrictions on the spread of the 2019 novel coronavirus (COVID-19) outbreak*, Science, 368:395–400, 2020.

[17] A. Cori, N. M. Ferguson, C. Fraser, and S. Cauchemez, *A new framework and software to estimate time-varying reproduction numbers during epidemics*, Am. J. Epidemiol., 178:1505–1512, 2013.

[18] G. Currie, T. Jain, and L. Aston, *Evidence of a post-COVID change in travel behaviour – Self-reported expectations of commuting in Melbourne*, Transp. Res. A: Policy Pract., 153:218–234, 2021.

[19] B. D. Dalziel, B. Pourbohloul, and S. P. Ellner, *Human mobility patterns predict divergent epidemic dynamics among cities*, Proc. R. Soc. B: Biol. Sci., 280:20130763, 2013.

[20] O. Diekmann, J. A. P. Heesterbeek, and J. A. J. Metz, *On the definition and the computation of the basic reproduction ratio R0 in models for infectious-diseases in heterogeneous populations*, J. Math. Biol., 28:365–382, 1990.

[21] O. Diekmann, J. Heesterbeek, and M. G. Roberts, *The construction of next-generation matrices for compartmental epidemic models*, J. R. Soc. Interface, 7:873–885, 2010.
[22] A. d'Onofrio and P. Manfredi, *Information-related changes in contact patterns may trigger oscillations in the endemic prevalence of infectious diseases*, J. Theor. Biol., 256:473–478, 2009.
[23] A. d'Onofrio and P. Manfredi, *Behavioral SIR models with incidence-based social-distancing*, Chaos Solit. Fractals, 159:112072, 2022.
[24] A. d'Onofrio, P. Manfredi, and E. Salinelli, *Vaccinating behaviour, information, and the dynamics of SIR vaccine-preventable diseases*, Theor. Popul. Biol., 71:301–317, 2007.
[25] E. Du, E. Chen, J. Liu, and C. Zheng, *How do social media and individual behaviors affect epidemic transmission and control?*, Sci. Total Environ., 761:144114, 2021.
[26] C. Fraser, *Estimating individual and household reproduction numbers in an emerging epidemic*, PLoS One, 2(8):e758, 2007.
[27] S. Funk, E. Gilad, C. Watkins, and V. A. Jansen, *The spread of awareness and its impact on epidemic outbreaks*, Proc. Natl. Acad. Sci. USA, 106:6872–6877, 2009.
[28] S. Funk, M. Salathé, and V. A. Jansen, *Modelling the influence of human behaviour on the spread of infectious diseases: A review*, J. R. Soc. Interface, 7:1247–1256, 2010.
[29] K. M. Gostic et al., *Practical considerations for measuring the effective reproductive number, R_t*, PLoS Comput Biol., 16(12):e1008409, 2020.
[30] D. Greenhalgh, *Hopf bifurcation in epidemic models with a latent period and nonpermanent immunity*, Math. Comput. Modelling, 25:85–107, 1997.
[31] Y.-H. Hsieh, P. Van den Driessche, and L. Wang, *Impact of travel between patches for spatial spread of disease*, Bull. Math. Biol., 69:1355–1375, 2007.
[32] Y. Jin and W. Wang, *The effect of population dispersal on the spread of a disease*, J. Math. Anal. Appl., 308:343–364, 2005.
[33] K. Khan et al., *Spread of a novel influenza A (H1N1) virus via global airline transportation*, N. Engl. J. Med., 361(2):212–214, 2009.
[34] D. Lacitignola and G. Saccomandi, *Managing awareness can avoid hysteresis in disease spread: An application to coronavirus COVID-19*, Chaos Solit. Fractals, 144:110739, 2021.
[35] M. N. Lessani, Z. Li, F. Jing, S. Qiao, J. Zhang, B. Olatosi, and X. Li, *Human mobility and the infectious disease transmission: A systematic review*, Geo-Spat. Inf. Sci., 27:1824–1851, 2024.
[36] M. Lu, D. Gao, J. Huang, and H. Wang, *Relative prevalence-based dispersal in an epidemic patch model*, J. Math. Biol., 86:52, 2023.
[37] Z. Ma and J. Li, *Dynamical Modeling and Analysis of Epidemics*, World Scientific, 2009.
[38] Z. Ma, Y. Zhou, and J. Wu, *Modeling and Dynamics of Infectious Diseases*, in: Series in Contemporary Applied Mathematics, Vol. 11, World Scientific, 2009.
[39] N. MacDonald, *Time Lags in Biological Models*, in: Lecture Notes in Biomathematics, Vol. 27, Springer Science & Business Media, 2013.
[40] P. Manfredi and A. D'Onofrio, *Modeling the Interplay Between Human Behavior and the Spread of Infectious Diseases*, Springer Science & Business Media, 2013.
[41] M. Martcheva, *An Introduction to Mathematical Epidemiology*, in: Texts in Applied Mathematics, Vol. 61, Springer, 2015.
[42] S. Meloni, N. Perra, A. Arenas, S. Gómez, Y. Moreno, and A. Vespignani, *Modeling human mobility responses to the large-scale spreading of infectious diseases*, Sci. Rep., 1:62, 2011.
[43] A. K. Misra, A. Sharma, and J. Shukla, *Modeling and analysis of effects of awareness programs by media on the spread of infectious diseases*, Math. Comput. Modelling Math. Comput. Modelling, 53:1221–1228, 2011.
[44] J. D. Murray, *Mathematical Biology: I. An Introduction*, in: Interdisciplinary Applied Mathe-

matics, Vol. 17, Springer Science & Business Media, 2007.
[45] K. Nelson, K. Marienau, C. Schembri, and S. Redd, *Measles transmission during air travel, United States, December 1, 2008–December 31, 2011*, Travel Med. Infect. Dis., 11:81–89, 2013.
[46] S. Ruan, W. Wang, and S. A. Levin, *The effect of global travel on the spread of ARS*, Math. Biosci. Eng., 3:205–218, 2005.
[47] C. Sun, W. Yang, J. Arino, and K. Khan, *Effect of media-induced social distancing on disease transmission in a two patch setting*, Math. Biosci., 230:87–95, 2011.
[48] G. Sun, Z. Jin, and A. Mai, *Dynamics of a two-patch SIR model with disease surveillance mediated infection force*, Commun. Nonlinear Sci. Numer. Simul., 132:107872, 2024.
[49] G. Sun, A. Mai, and Z. Jin, *Modeling precaution, immunity loss and dispersal on disease dynamics: A two-patch SIRS model*, Adv. Contin. Discrete Models, 2025:3, 2025.
[50] S. Tang, Y. Xiao, Y. Yang, Y. Zhou, J. Wu, and Z. Ma, *Community-based measures for mitigating the 2009 H1N1 pandemic in China*, PLoS ONE, 5:e10911, 2010.
[51] P. van den Driessche and J. Watmough, *Reproduction numbers and sub-threshold endemic equilibria for compartmental models of disease transmission*, Math. Biosci., 180:29–48, 2002.
[52] W. Wang and G. Mulone, *Threshold of disease transmission in a patch environment*, J. Math. Anal. Appl., 285:321–335, 2003.
[53] W. Wang and X.-Q. Zhao, *An epidemic model in a patchy environment*, Math. Biosci., 190:97–112, 2004.
[54] Z. Wang, C. T. Bauch, S. Bhattacharyya, A. d'Onofrio, P. Manfredi, M. Perc, N. Perra, M. Salathé, and D. Zhao, *Statistical physics of vaccination*, Phys. Rep., 664:1–113, 2016.
[55] A. Wilder-Smith, *The severe acute respiratory syndrome: Impact on travel and tourism*, Travel Med. Infect. Dis., 4:53–60, 2006.
[56] M. E. Wilson, *Travel and the emergence of infectious diseases*, Emerg. Infect. Dis., 1:39, 1995.
[57] W. Yang, C. Sun, and J. Arino, *Effect of media-induced modification of travel rates on disease transmission in a multiple patch setting*, J. Appl. Anal. Comput., 10:2682–2703, 2020.
[58] Y. Yang, J. Wu, J. Li, and Z. Ma, *Global dynamics – convergence to equilibria – of epidemic patch models with immigration*, Math. Comput. Modelling, 51:329–337, 2010.
[59] C. Zuo, F. Zhu, and Y. Ling, *Analyzing COVID-19 vaccination behavior using an SEIRM/V epidemic model with awareness decay*, Front. Public Health, 10:817749, 2022.